

Preference is More Than Comparisons: Rethinking Dueling Bandits with Augmented Human Feedback

Shengbo Wang¹, Hong Sun¹, Ke Li²

¹School of Computer Science and Engineering, University of Electronic Science and Technology of China, Chengdu, China

²Department of Computer Science, University of Exeter, EX4 4RN, Exeter, UK

shnbo.wang@foxmail.com; k.li@exeter.ac.uk

Abstract

Interactive preference elicitation (IPE) aims to substantially reduce human effort while acquiring human preferences in wide personalization systems. Dueling bandit (DB) algorithms enable optimal decision-making in IPE building on pairwise comparisons. However, they remain inefficient when human feedback is sparse. Existing methods address sparsity by heavily relying on parametric reward models, whose rigid assumptions are vulnerable to misspecification. In contrast, we explore an alternative perspective based on feedback augmentation, and introduce critical improvements to the model-free DB framework. Specifically, we introduce augmented confidence bounds to integrate augmented human feedback under generalized concentration properties, and analyze the multi-factored performance trade-off via regret analysis. Our prototype algorithm achieves competitive performance across several IPE benchmarks, including recommendation, multi-objective optimization, and response optimization for large language models, demonstrating the potential of our approach for provably efficient IPE in broader applications.

Code — <https://github.com/COLA-Laboratory/IPEA-HF>

1 Introduction

In personalization systems ranging from recommendation (Austin et al. 2024) and multi-objective optimization (Huang, Wang, and Li 2024) to large language models (LLMs) (Rafailov et al. 2023), acquiring user preferences is essential but often incurs great human effort. Interactive preference elicitation (IPE) has the potential to substantially reduce this burden by selectively querying users through iterative strategies (Xiong et al. 2024). Building on pairwise comparisons, the dueling bandit (DB) framework has evolved into a strong theoretical foundation for IPE over the past decade (Yue et al. 2012; Zoghi et al. 2014; Saha 2021). However, even under optimal strategies, the DB framework struggles to maintain efficiency in the presence of sparse feedback, leading to waning research attention and limited practical adoption in recent years. As a result, while personalization systems continue to demand data-efficient interaction, achieving *provably efficient* IPE remains a pressing challenge.

Copyright © 2026, Association for the Advancement of Artificial Intelligence (www.aaai.org). All rights reserved.

Sparse feedback in practice often reveals a deeper insight: human preferences are more than isolated pairwise comparisons. They are also shaped by cues such as contextual information and latent dependencies (Sun et al. 2024). The independent treatment of human feedback in the DB framework may be a key source of its inefficiency. Augmenting human feedback with these cues could pave the way for a more effective DB framework that better facilitates IPE. Preliminary efforts in this direction have primarily relied on parametric preference models, most notably the Bradley–Terry (BT) model (Bradley and Terry 1952). However, while such model assumptions are convenient and analytically tractable, they have been increasingly criticized for their susceptibility to model misspecification (Heckel et al. 2016; Verma et al. 2025) and suboptimal performance in the presence of non-transitive preferences (Munos et al. 2024). Alternative methods that exploit contextual information and dependencies do exist but have yet to form a widely applicable framework (Sui et al. 2017; Xiao et al. 2025). Furthermore, several fundamental questions about the DB framework with augmented human feedback remain unaddressed. In this work, we focus on the following three research questions (RQs):

RQ1: *How can the DB framework integrate and interpret the role of augmented human feedback, while reducing reliance on rigid, predefined model assumptions?*

In the broader framework of contextual bandits (Lattimore and Szepesvári 2020), side information can be exploited through various approaches, including structured reward estimation, candidate partitioning, or similarity-based methods. Algorithms based on parametric BT models, for instance, typically fall under the reward estimation category. As discussed earlier, reward estimation risks model misspecification and struggles to accommodate non-transitive preferences. Alternatively, candidate partitioning offers favorable regret bounds that scale with the number of partition groups (Huang, Wang, and Li 2024). However, it relies on a strong assumption that candidates can be cleanly divided into distinguishable subsets, an assumption often unverifiable in real-world settings. In this work, we explore similarity-based methods to integrate augmented human feedback. While closely related to other approaches (Slivkins 2014), such methods remain largely underexplored with respect to their efficiency in IPE (Sui et al. 2017). Our methodology is motivated by extending the concentration results of the context-free DB framework

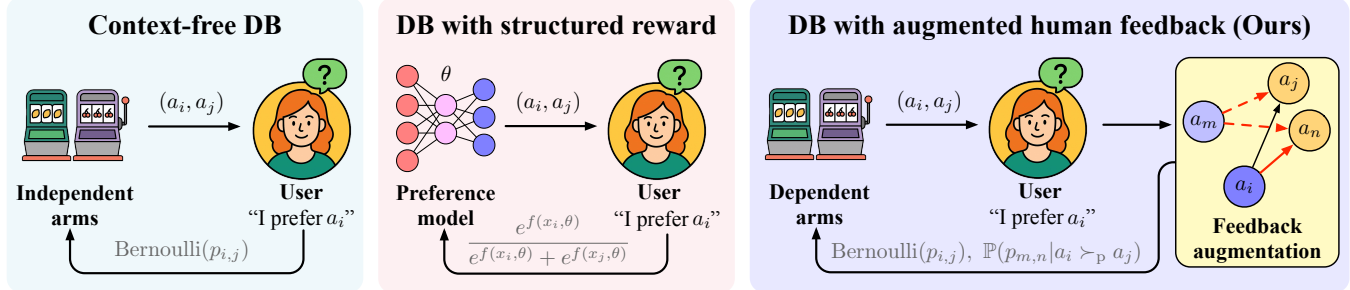


Figure 1: Comparison of three DB approaches: context-free DB, structured reward estimation, and DB with augmented feedback.

(Zoghi et al. 2014). We conclude that augmenting human feedback serves as a mechanism for uncertainty calibration, offering a unifying perspective across various DB approaches. A comparison of DB approaches is presented in Figure 1.

RQ2: *Does the incorporation of augmented human feedback consistently improve the efficiency of DB algorithms, or can it sometimes introduce performance degradation?*

Existing studies on augmented human feedback, typically grounded in parametric or distinguishable assumptions, have shown considerable promise in improving sample efficiency. However, they often struggle to explain common pitfalls such as overfitting (Azar et al. 2024) and optimization inefficiencies (Razin et al. 2025). By discarding these predefined assumptions, we open the black box of feedback augmentation, enabling a deeper investigation into how augmented human feedback influences decision-making within the DB framework. Following the upper confidence bound (UCB) method (Srinivas et al. 2010), we provide theoretical analysis of sample complexity and regret bounds, revealing an explicit trade-off governed by multiple factors. These findings provide practical guidance on when to leverage, how to calibrate, and what to explore regarding human feedback augmentation, positioning the DB framework as a stronger foundation for subsequent IPE algorithm design and evaluation.

RQ3: *Can the DB framework be extended beyond pairwise comparisons to incorporate richer forms of human feedback, thereby establishing a more general foundation for IPE?*

Most IPE approaches, including augmented variants of the DB framework, are constrained to receiving human preferences exclusively through pairwise comparisons. However, incorporating richer forms of human feedback, such as feature-level comparisons (Austin et al. 2024), expert demonstrations (Sun et al. 2024), and explanations of human choice (Ghazimatin et al. 2021), has been shown to positively influence decision-making efficiency. As diverse feedback sources become increasingly available, the standard DB framework remains limited in its ability to directly utilize such information. Fortunately, our DB framework offers the potential to integrate heterogeneous forms of human feedback beyond pairwise comparisons. This is achieved by treating all feedback as a unified signal that characterizes contextual similarity and dependencies among candidates. Ultimately, this would provide a more flexible foundation for IPE tasks.

We highlight the following key advances in this work:

- We develop a model-free DB framework with a general-

ized concentration property, enabling the integration of augmented human feedback and the quantification of its influence. Our framework connects human feedback to the calibration of confidence bounds, aligning in mechanism with a broad class of DB approaches.

- We study the sample complexity and cumulative regret bounds in the proposed DB framework, revealing an explicit trade-off between the amount of augmented human feedback and the strength of contextual dependencies. In addition, our analysis includes partition-based approaches (Huang, Wang, and Li 2024) as a special case.
- We present prototype designs that incorporate a similarity-based graph structure and an auxiliary annotation process for capturing contextual dependencies. Our algorithms demonstrate competitive performance across several benchmarks, including recommendation, multi-objective optimization, and LLM response optimization.

2 Problem Formulation

We consider an IPE task involving K ($K \geq 2$) candidates, where the goal is to identify the candidate that best aligns with the user's preference, typically inferred through pairwise comparisons. Mathematically, the task can be formulated as a K -arms DB problem, where the set of arms is indexed by $\mathcal{A} = \{1, 2, \dots, K\}$. When contextual information is available, each arm a_i is associated with a context vector $x_i \in \mathcal{X}$. In the t -th round, the user is asked to evaluate a pair of arms (a_i, a_j) , where $i, j \in \mathcal{A}$ and $i \neq j$. The user should decide, based on her/his preferences, whether a_i is better, worse, or equivalent to a_j , denoted as $a_i \succ_p a_j$, $a_i \prec_p a_j$, or $a_i \simeq_p a_j$. For stochastic preferences, we assume a fixed preference matrix $\mathbf{P} = [p_{i,j}]_{K \times K}$, where $p_{i,j}$ denotes the probability that arm a_i is preferred over arm a_j (Yue et al. 2012). Without loss of generality, we have $p_{i,j} + p_{j,i} = 1$ and $p_{i,i} = 0.5$. An arm a_i is said to be superior to the a_j if $p_{i,j} > 0.5$. We also denote the best candidate as the winner a_* , defined by criteria such as the Condorcet or Copeland winners (Urvoy et al. 2013), among all arms.

The *context-free* DB framework maintains a winning matrix $\mathbf{B} = [b_{i,j}]_{K \times K}$ to record the pairwise comparison labels, where $b_{i,j}$ denotes the number of times when arm a_i is preferred over arm a_j . The estimated preference probability with mean $\tilde{p}_{i,j} = \frac{b_{i,j}}{b_{i,j} + b_{j,i}}$, and the upper confidence bound (UCB) $\mathbf{U} = [\tilde{u}_{i,j}]_{K \times K}$ and lower confidence bound (LCB)

$\mathbf{L} = [\tilde{l}_{i,j}]_{K \times K}$ are given by (Zoghi et al. 2014):

$$\tilde{u}_{i,j} = \tilde{p}_{i,j} + \sqrt{\frac{\alpha \log t}{b_{i,j} + b_{j,i}}}, \quad \tilde{l}_{i,j} = \tilde{p}_{i,j} - \sqrt{\frac{\alpha \log t}{b_{i,j} + b_{j,i}}}, \quad (1)$$

where $\alpha > 0$ controls the confidence interval, and t is the total number of comparisons so far. Consequently, all arms are treated independently according to their own labels.

To encode contextual information and dependencies (Lattimore and Szepesvári 2020), a common DB approach is based on structured reward estimation. This approach assumes a structured form for $p_{i,j}$, such as the BT model, and a parametric reward function $f(x_i, x_j) = \theta^\top (x_i - x_j)$, with the unknown parameter θ to be determined:

$$\tilde{p}_{i,j}(x_i, x_j) = \frac{1}{1 + \exp(-f(x_i, x_j))}, \quad x_i, x_j \in \mathcal{X}. \quad (2)$$

This formulation transforms the problem of identifying the best arm into one of learning the unknown parameter θ . Despite its favorable sample complexity, both the probability structure and parametric reward assumptions have been called into question (Heckel et al. 2016; Verma et al. 2025; Munos et al. 2024; Azar et al. 2024; Razin et al. 2025).

Another way to leveraging contextual information is through candidate partitioning, such as clustering (Huang, Wang, and Li 2024), merging (Li et al. 2020), or team grouping (Cohen, Schmidt-Kraepelin, and Mansour 2021). These methods partition the K arms into C subsets, where $C < K$ in order to improve sample efficiency. The partitioning process is often based on the assumption that all arms within the winner subset are strictly superior to those in other subsets (Jedor, Perchet, and Louëdec 2019), a property we referred to as *distinguishability*. However, candidate partitioning in real-world IPE may not always guarantee such property. A more robust alternative is to model dependencies through similarity (Sui et al. 2017). Let $s : \mathcal{X} \times \mathcal{X} \rightarrow [0, 1]$ denote a similarity function. The special case where $s \in \{0, 1\}$ corresponds to settings satisfying the distinguishable property. Nevertheless, the sample efficiency based on similarity remains unclear. We will explore this gap in the subsequent sections.

In this work, we consider the Condorcet winner (Yue et al. 2012) for both analytical convenience and consistent benchmarking across different DB approaches. Specifically, the probability of a_* satisfies $p_{*,j} > 1/2, \forall j \in \mathcal{A} \setminus \{*\}$. If a_i and a_j were chosen for comparison at time t , the instantaneous regret is defined as $r_t = \frac{\Delta_i + \Delta_j}{2}$, where $\Delta_k = p_{*,k} - \frac{1}{2}$, $\forall k \in \mathcal{A}$. Accordingly, in the context of DB, the objective of IPE is to minimize the *cumulative regret up to time T* , defined as $R(T) = \sum_{t=1}^T r_t$. The equivalence of regret measures for parametric DB approach is demonstrated in (Saha 2021).

3 Method

In this section, we delineate the DB framework for IPE with augmented human feedback, referred to as IPEA-HF. The overall structure is outlined in Algorithm 1, which compromises four key components. It begins by introducing augmented confidence bounds that incorporate augmented human feedback in a model-free setting. This is followed by

Algorithm 1: Pseudo-code of IPEA-HF

Input: Candidate number K , context set \mathcal{X} , $\alpha > 0$
Init: $\mathbf{B} = [0]_{K \times K}$, graph $\mathcal{G}(\mathcal{X}, K)$, $W = [0]$.
repeat
 $\mathbf{U}, \mathbf{L} \leftarrow \text{AugConfidanceBound}(\mathbf{B}, \mathcal{G}, W, \alpha)$
 Select pairs (a_i, a_j) $\leftarrow \text{DuelingBanditAlgo}(\mathbf{U}, \mathbf{L})$
 Observe $a_{\text{win}}, a_{\text{lose}}$ and update $b_{\text{win,lose}} \leftarrow b_{\text{win,lose}} + 1$
 $W \leftarrow \text{DependencyExtract}(\mathcal{X}, \mathcal{G}, W)$
 $\mathcal{G} \leftarrow \text{FeedbackAug}(a_{\text{win}}, a_{\text{lose}}, W, \mathcal{G})$
until IPE task finished or budget exhausted

pair selection criteria, which depend on the specific DB algorithm employed, such as the relative upper confidence bound (RUCB) (Zoghi et al. 2014) or double Thompson sampling (DTS) (Wu and Liu 2016). Upon observing a user response, IPEA-HF augments the feedback based on contextual similarity and extracted dependencies through computational algorithm designs and additional annotations.

3.1 AugConfidanceBound: Integrating Confidence Bounds with Augmented Feedback

The confidence bounds in the DB framework play a pivotal role in determining which pairs are selected for comparison, and ultimately shape the overall query process. As formalized in equation (1), bounds $\tilde{u}_{i,j}$ and $\tilde{l}_{i,j}$ in the context-free DB approach rely solely on *direct* observations from comparisons between the pair (a_i, a_j) , specifically the counts $b_{i,j}$ and $b_{j,i}$. In contrast, we explore whether incorporating additional *related* observations from augmented human feedback can enhance the estimation of confidence bounds. For $i, j \in \mathcal{A}$, let $n_{i,j}^d(t) = b_{i,j} + b_{j,i}$ denote the number of direct comparisons between a_i and a_j up to time t , and let $n_{i,j}^r(t)$ denote the number of related observations inferred from other pairwise comparisons up to time t . We then define the total observation count as $n_{i,j}(t) = n_{i,j}^d(t) + n_{i,j}^r(t)$. The augmented mean becomes $\hat{p}_{i,j} = \frac{1}{\eta n_{i,j}(t)} \left(b_{i,j} + \sum_{k=1}^{n_{i,j}^r} X_{i,j}^k \right)$, and the UCB and LCB take the following form:

$$\hat{u}_{i,j} = \hat{p}_{i,j} + \frac{1}{\eta} \sqrt{\frac{\alpha \ln t}{n_{i,j}(t)}}, \quad \hat{l}_{i,j} = \hat{p}_{i,j} - \frac{1}{\eta} \sqrt{\frac{\alpha \ln t}{n_{i,j}(t)}}. \quad (3)$$

where $\eta = (n_{i,j}^d + \sum_{k=1}^{n_{i,j}^r} w_{i,j}^k) / n_{i,j}$ with $w_{i,j}^k \in [0, 1]$ to be determined, and $X_{i,j}^k$ denotes a random variable in $[0, 1]$ determined by related observations. By definition, without augmented feedback, i.e., $n_{i,j}^r = 0$, the augmented confidence bounds reduce to model-free ones in equation (1).

Concentration property We provide the following concentration property of the augmented confidence bounds as a generalized result from the context-free DB framework (Zoghi et al. 2014; Wu and Liu 2016).

Theorem 3.1. *Assume $X_{i,j}^k \sim \text{Bernoulli}(w_{i,j}^k p_{i,j})$ and let $C(\delta) = \left(\frac{(4\alpha-1)K^2}{(2\alpha-1)\delta} \right)^{\frac{1}{2\alpha-1}}$. Given the preference matrix \mathbf{P}*

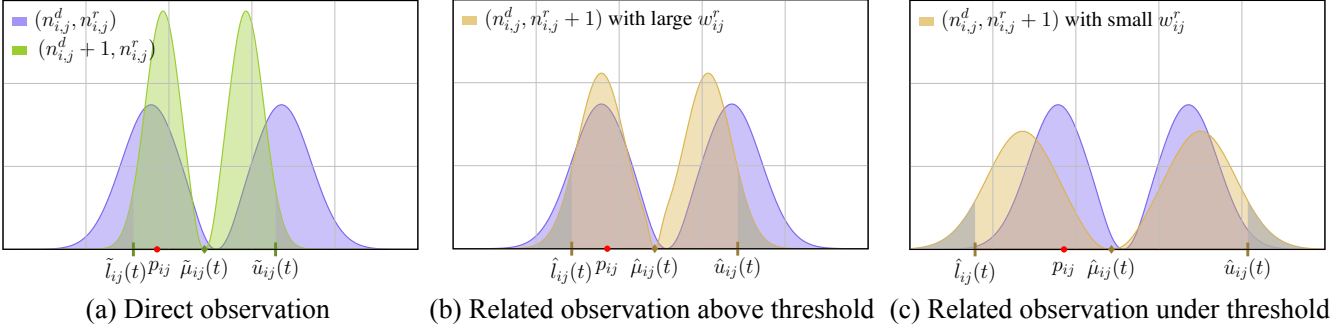


Figure 2: Comparison of confidence intervals adding a direct observation or a related observation. The curve shows the derivative of the bound in equation (4), where the shaded area is the probability that the confidence interval fails to contain $p_{i,j}$.

with K arms, then, for any $\alpha > 0.5$ and $\delta \in (0, 1)$, we have:

$$P\left(\forall t > C(\delta), i, j \in \mathcal{A}, p_{i,j} \in [\hat{l}_{i,j}(t), \hat{u}_{i,j}(t)]\right) > 1 - \delta. \quad (4)$$

The proof is given in Appendix 11.1. This result suggests that additional observations can be leveraged to inform the estimation of confidence bounds in conjunction with the latent dependency weight $w_{i,j}^k$. We will later discuss how to obtain the weights in Section 3.3.

We now study the property of concentration. Consider the case where $n_{i,j}^r(t) = 0$. Given a direct observation, the confidence interval shrinks from $\sqrt{\alpha \ln t / n_{i,j}^d(t)}$ to $\sqrt{\alpha \ln t / (n_{i,j}^d(t) + 1)}$. The confidence intervals progressively narrow as the number of direct comparisons increases (Zoghi et al. 2014). By contrast, for a related observation, the confidence bound takes the form $\frac{1}{\eta} \sqrt{\alpha \ln t / (n_{i,j}^d(t) + 1)}$. Notably, the weighting term $w_{i,j}^k$ influences the behavior of the confidence bound. When $w_{i,j}^r = 1$, we have $\eta = 1$, and the confidence bound shrinks in the same way as with a direct observation. Conversely, when $w_{i,j}^r = 0$, the bound becomes $\sqrt{\alpha(n_{i,j}^d(t) + 1) \ln t / n_{i,j}^{d,2}(t)}$, which is strictly larger than the original bound $\sqrt{\alpha \ln t / n_{i,j}^d(t)}$. Therefore, both direct and relative observations contribute to the *uncertainty calibration* for the confidence bounds, with the effect of relative observations depending on the strengths of dependencies.

Calibration threshold When estimating $p_{i,j}$, a smaller confidence interval is desirable for making more informed decisions. We can quantify the impact of augmented feedback by the ratio of confidence intervals with and without a relative observation:

$$\begin{aligned} \frac{\hat{u}_{i,j} - \hat{l}_{i,j}}{\tilde{u}_{i,j} - \hat{l}_{i,j}} &= \frac{1}{\eta} \sqrt{\frac{\alpha \ln t}{n_{i,j}^d(t) + 1}} / \sqrt{\frac{\alpha \ln t}{n_{i,j}^d(t)}} \\ &\in \left[\sqrt{1 - \frac{1}{n_{i,j}^d(t) + 1}}, \sqrt{1 + \frac{1}{n_{i,j}^d(t)}} \right]. \end{aligned} \quad (5)$$

We can derive a threshold condition for identifying *good* feedback augmentation that facilitates uncertainty calibration:

$$w_{i,j}^r > \eta n_{i,j}(t) \left(\sqrt{1 + \frac{1}{n_{i,j}(t)}} - 1 \right). \quad (6)$$

This condition holds for all $n_r \geq 0$. The detailed derivation is provided in Appendix 11.2. The result indicates that the contribution of a relative observation increases monotonically with the strength of $w_{i,j}^r$, becomes equivalent to a direct observation when $w_{i,j}^r = 1$, and diminishes as the number of direct observations increases, as illustrated in Figure 2.

Connections to other DB approaches The augmented confidence bounds naturally encompass partition-based approaches as a special case. Specifically, for all arms within a distinguishable group, related observations correspond to complete dependencies, i.e., $w_{i,j}^r = 1$. By considering only related observations within the same group, the comparison between individual arms effectively reduces to a comparison between groups, mirroring the operations adopted in partition-based approaches. For DB approaches with structured reward, they maintain a pairwise score of the form $u_f(x_i, x_j) = \hat{\theta}(x_i - x_j) + \sigma \|x_i - x_j\|_{V^{-1}}$ where $\hat{\theta}$ is the estimated parameter, $\sigma > 0$, and V is the sum of outer products of compared pairs (Verma et al. 2025; Saha 2021). The second term of $u_f(x_i, x_j)$ represents the confidence bound expressed as a Mahalanobis norm (Mahalanobis and 1936). For a pair (a_i, a_j) , more frequent comparisons, i.e., more direct observations in our setting, assign smaller weight to the direction of $x_i - x_j$. Given a related observation that is close in distance to (a_i, a_j) , representing stronger dependencies, the weight is further reduced along that direction, indicating a narrowed uncertainty calibration for the score of (a_i, a_j) . This mechanism that lowers the direction weight in the presence of high-correlated observations aligns with our proposed method. However, the confidence bound in structured reward approaches remains heuristic and lacks formal guarantees on the concentration property (i.e., $p_{i,j}$ may not be included within the bound with high probability as t increases beyond a certain threshold), making it prone to overfitting due to model misspecification.

Insights on RQ1: By leveraging the generalized concentration property, our method fundamentally strengthens the model-free DB framework by incorporating related observations into the estimation of winning probabilities and confidence bounds. We identify the key conditions under which contextual correlations enhance uncertainty calibration and establish clear connections to structured and partition-based approaches, highlighting the broader applicability.

3.2 DuelingBanditAlgo: Decision-Making with Augmented Feedback

The estimation of winning probabilities and their confidence bounds is integrated into DB decision-making algorithms to strike a balance between *exploitation* and *exploration*. These algorithms select candidate pairs through a two-stage process:

1. (Exploitation) Select the most promising arm as the first candidate. This is achieved by identifying the arm whose UCBs outperform the largest number of other arms.
2. (Exploration) Select the most competitive arm against the first candidate. This aims to identify the arm likely to beat the first selected arm according to their UCB and LCB.

Existing DB algorithms differ in their selection mechanism, including both deterministic and stochastic strategies, such as RUCB (Zoghi et al. 2014) and DTS (Wu and Liu 2016). Our augmented confidence bounds can be seamlessly integrated into both types. We propose two DB algorithms: IPEA-RUCB and IPEA-DTS integrated with augmented confidence bounds, with detailed descriptions in Appendix 8.

Sample Efficiency Following the analysis in (Zoghi et al. 2014), we investigate the RUCB variant integrated with augmented confidence bounds. Since our framework incorporates both direct observations (real samples) and related observations (virtual samples), the following result establishes a high-probability bound on the total sample complexity of each suboptimal arm pair.

Theorem 3.2. *Given the setup in Theorem 3.1, and let $D_{i,j}^w = \frac{4\alpha}{\min_r w_{i,j}^r \min\{\Delta_i^2, \Delta_j^2\}}$. For the IPEA-RUCB algorithm and any suboptimal pair $(a_i, a_j) \neq (a_*, a_*)$, $n_{i,j}(t)$ satisfies*

$$P(\exists t, i, j \in \mathcal{A}, n_{i,j}(t) > C(\delta) \vee D_{i,j}^w \ln t) < \delta. \quad (7)$$

The proof is given in Appendix 11.3. Accordingly, the multi-factored sample complexity reveals a fundamental **trade-off** in integrating augmented feedback. On the positive side, for a pair (a_i, a_j) that utilizes related observations of (a_m, a_n) , it holds that $n_{i,j}^d(t) + n_{m,n}^d(t) \leq n_{i,j}(t)$. That is, the number of direct observations of one pair that provide augmented feedback to other pairs is already included in the total sample count of the latter. If more pairs are related, the total sampling count satisfies $n_{i,j}^d(t) + \sum_{m,n} n_{m,n}^d(t) \leq n_{i,j}(t)$. This indicates that incorporating related observations has the potential to improve overall sample efficiency. However, for less dependent observations, e.g., when $\min_r w_{i,j}^r \rightarrow 0$, $D_{i,j}^w$ can increase significantly, introducing a large coefficient into the overall sample complexity. According to this trade-off,

augmented feedback should be integrated selectively, prioritizing observations with strong contextual dependencies.

Regret Analysis To conduct regret analysis, we assume bidirectional dependency: if a pair (a_i, a_j) utilizes related observations from another pair (a_m, a_n) , the latter also utilizes the observations from (a_i, a_j) . A direct consequence of this assumption is the soft-clustering, grouping candidates into C subsets. Notably, existing methods based on distinguishability (Li et al. 2020; Cohen, Schmidt-Kraepelin, and Mansour 2021) or arm dependencies (Sui et al. 2017) satisfy this assumption. Furthermore, our method generalizes beyond these settings, as illustrated by the diverse cases in Figure 3.

Theorem 3.3. *Follow the setup in Theorems 3.1 and 3.2 and assume bidirectional dependencies. If we have C soft clusters and each cluster contains K_i candidates, the cumulated regret bound of IPEA-RUCB is $\mathcal{O}\left(\frac{1}{\min_{i,j,r} w_{i,j}^r} \hat{K}^2 \log T\right)$, where $\hat{K} = \max\{C, K_1, \dots, K_C\}$.*

The proof is provided in Appendix 11.4. This result subsumes the partition-based DB approach as a special case. For example, the cluster-based DB method achieves a regret bound of $\mathcal{O}(C^2 \log T)$ (Huang, Wang, and Li 2024), where the analysis is conducted at the cluster level under the assumption of distinguishability ($w_{i,j}^r \equiv 1$). In contrast, our result operates at the candidate level and explicitly accounts for varying degree of dependency, such that the candidate count in each subset is also reflected in the effective parameter \hat{K} . In conclusion, our regret bound generalizes the partition-based approach (Huang, Wang, and Li 2024) and offers promising support for DB algorithms that incorporate correlations or dependent arms (Sui et al. 2017).

Insights on RQ2: *Our analysis of sample complexity and regret bounds reveals a fundamental trade-off in incorporating augmented human feedback into DB algorithms. Theoretical results consistently show that related observations with strong dependencies can substantially reduce the number of required interactions, thereby improving efficiency. This finding aligns with existing conclusions and offers generalized support to model-free, dependency-aware DB approaches.*

3.3 DependencyExtract & FeedbackAug: Computational Design

Our algorithm consists of two key components: extracting dependencies and augmenting human feedback. Our analysis (Theorem 3.1) characterizes latent dependencies as the joint distribution of direct and indirect observations, formalized as Bernoulli($w_{i,j}^k p_{i,j}$). The weighting term $w_{i,j}^k$ captures the conditional dependency between pairs.

To estimate $w_{i,j}^r$, we follow a two-step procedure, as illustrated in Figure 4. First, we construct a prior structural skeleton by building a similarity graph over the candidates, where the edges are determined by similarity distances in the context space \mathcal{X} . We filter out dissimilar pairs using graph partitioning or soft clustering, thereby concentrating on the most meaningful dependencies. As a result, each candidate

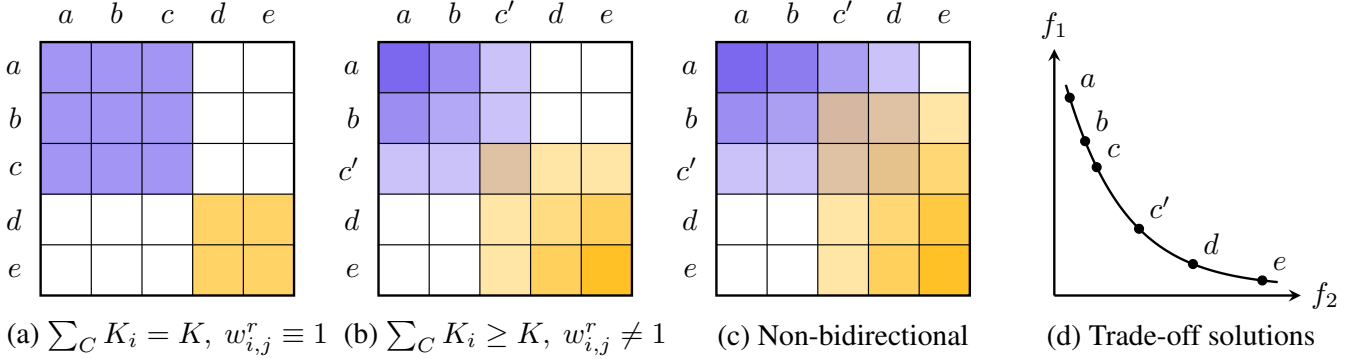


Figure 3: Illustrative cases for bidirectional dependency. (a) Candidate partitioning. (b) Dependent arms with symmetric correlations. (c) General case without bidirectional dependency. (d) Two-objective trade-off solutions whose dependencies are determined by their distances. Given $[a, b, c, d, e]$, the candidates can be safely grouped into two subsets. When c shifts to c' , the dependencies weaken, making soft clustering a more suitable choice.

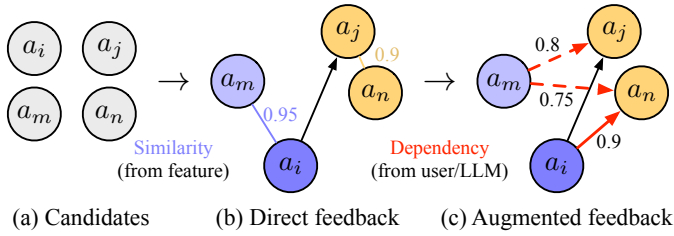


Figure 4: Illustration of computational design of dependency extraction and feedback augmentation.

is associated with one or more groups, depending on the employed partitioning method. At each round of pairwise comparisons, we observe human feedback on a pair, e.g., a_i is preferred over a_j . Then, we should determine the dependencies. Through additional annotations, we selectively query user or LLMs to annotate conditional dependencies over local pairwise relations, and incorporate related observations with high dependency scores into the DB loop. Specifically, we iterate over and combine all pairs from the groups associated with a_i and a_j . When a_i and a_j belong to the same group, no feedback augmentation is performed.

While the annotation process for dependency estimation provides valuable signals for feedback augmentation, it may introduce errors, particularly when relying on simulated annotators such as LLMs. The robustness of our framework stems from the fact that the influence of a related observation is strictly weaker than that of a direct observation, and further diminishes as the number of direct observations increases (see equation (5)). In addition, the impact of biased estimation in DB has been analyzed in (Yi, Kang, and Li 2024). As interactions accumulate, the estimated dependencies are either refined or discarded, enabling the algorithm to recover from initial noisy annotations over time.

Richer Forms of Human Feedback In the modelling of conditional dependencies, multiple forms of feedback can be leveraged. Beyond pairwise comparisons and contextual

similarities, our method also incorporates reasoning signals derived from LLMs or domain experts on latent contextual dependencies. Additional types of data, such as human explanations and rationales (Ghazimatin et al. 2021), can also be readily integrated, all contributing to the discovery and refinement of informative conditional dependencies. This enables the incorporation of richer feedback signals within a principled framework, supported by the theoretical foundations of our DB framework. As more dependency data becomes available, probabilistic graphical models can be employed to capture joint distributions and conditional structures, thereby further denoising sparse human feedback and estimating missing relationships.

4 Empirical Study

We evaluate our algorithms (IPEA–RUCB and IPEA–DTS) across a diverse set of benchmarks:

- **Item Recommendation.** We consider the Sushi dataset containing full rankings over 10 types of sushi collected from 5,000 customer orders (Kamishima and Akaho 2010), and a Car Preference dataset with full rankings over 10 cars provided by 60 U.S. users via Amazon Mechanical Turk (Abbasnejad et al. 2013).
- **Multi-Objective Optimization.** We adopt the *a posteriori* setting of preference-based evolutionary multi-objective optimization (PBEMO) (Huang, Wang, and Li 2024), considering the celebrated synthetic test problems (DTLZ2 and DTLZ7) with different landscapes (Deb et al. 2005).
- **LLM Response Optimization.** We follow the experimental settings in (Verma et al. 2025; Dwaracherla et al. 2024) to conduct *active exploration* given a pool of responses for each prompt sampled from Anthropic Helpfulness and Harmlessness (H-H) dataset (Bai et al. 2022).

We consider five state-of-the-art DB methods spanning context-free and parametric frameworks.

- **Context-free algorithms.** We include two prominent DB algorithms: Relative Upper Confidence Bound (RUCB) (Zoghi et al. 2014) and Double Thompson Sampling (DTS) (Wu and Liu 2016).

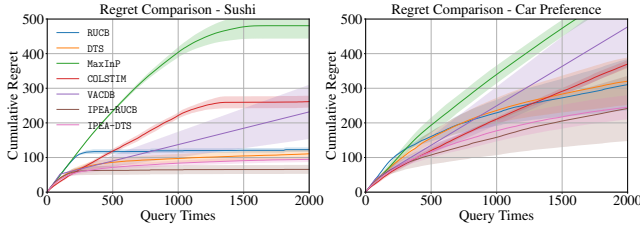


Figure 5: Regret trajectories on Sushi and Car Preference.

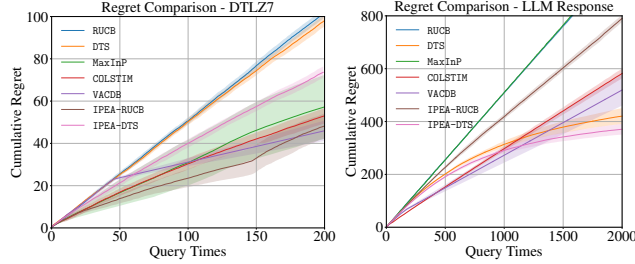


Figure 6: Regret on DTLZ7 and LLM Exploration.

- **Parametric algorithms.** We select three state-of-the-art methods based on the BT models: Maximum Informative Pair (MaxInP) (Saha 2021), COLSTIM (Bengs, Saha, and Hüllermeier 2022), and VACDB (Di et al. 2024).

Detailed experimental settings are given in Appendix 9.

Item Recommendation We simulate 2,000 interaction rounds to reflect the aggregated preferences of a user group. The cumulative regret of all algorithms is shown in Figure 5. Under a moderate number of candidate items, context-free DB algorithms consistently outperform parametric baselines. Building on this foundation, our proposed algorithms achieve further improvements in sample efficiency. The inferior performance of parametric methods is largely due to model misspecification, which is exacerbated when handling real-world, mixed-type feature spaces. Moreover, some parametric algorithms suffer from premature convergence. For example, VACDB exhibits a steadily increasing regret curve, indicating that it fails to maintain effective exploration over time.

Multi-Objective Optimization We simulate 200 interaction rounds to evaluate algorithm performance under sparse human feedback. The cumulative regret trajectories are shown in the left panel of Figure 6. As expected, the standard DB algorithms RUCB and DTS exhibit poor efficiency when facing a large candidate set (100^2 pairs) and a limited interaction budget. Although parametric DB algorithms demonstrate relatively better performance, their limitations are evident. Regarding the query frequency as given in Figure 7, both COLSTIM and VACDB repeatedly select a small subset of pairs, reflecting strong exploitation and a lack of sufficient exploration. In contrast, our proposed algorithms achieve a better trade-off between regret minimization and query diversity. Notably, IPEA-RUCB performs more favorably than IPEA-DTS under these conditions, suggesting that deterministic strategies may be more robust to sparse feedback.

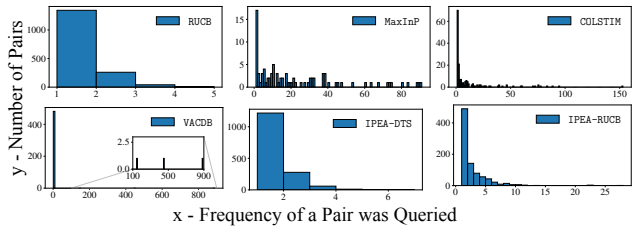


Figure 7: Analysis of Query frequency on the DTLZ7 task. In the histogram, (2, 1000) denotes 1,000 unique pairs each queried twice. A broader spread at low frequencies indicates greater exploration.

Response Optimization The regret trajectories are shown in the right panel of Figure 6. Most algorithms exhibit a degree of inefficiency, with the exception of DTS and IPEA-DTS, both employ a stochastic strategy. This aligns with the empirical findings of (Dwaracherla et al. 2024), where DTS was shown to be the most effective algorithm for active exploration for LLMs. Notably, by integrating augmented human feedback, our algorithms consistently outperform their context-free counterparts, RUCB and DTS. In contrast, algorithms based on parametric models require significantly more computational resource, due to the high dimensionality of the embedded feature space (768 dimensions from the MPNet (Song et al. 2020)). As a result, without a dedicated context-aware mechanism (Verma et al. 2025), the effectiveness using parametric DB for response optimization remains questionable.

In response optimization, our algorithms leverage not only related observations from the same prompt but also inter-prompt observations with high contextual similarity and dependency. This pilot demonstration shows the effectiveness of feedback augmentation beyond pairwise comparisons.

Insights on RQ3: *By treating human feedback as unified signals characterizing contextual similarity and dependencies, our prototype computation designs are readily extensible to incorporate richer forms of feedback. In our experiments, we integrate contextual similarity, LLM-powered dependency annotations, and inter-prompt observations, each serving as an additional form of human feedback. This expands the applicability of the DB framework, offering a promising pathway for adapting to diverse feedback modalities in future IPE tasks.*

5 Conclusions

We introduced a novel DB framework that integrates augmented human feedback to enable provably efficient IPE. By analyzing the concentration properties and performance trade-offs, we demonstrated the effectiveness of feedback augmentation and established connections to a broad class of existing DB approaches. In addition, we proposed prototype computational designs that incorporate richer forms of human feedback, and showed competitive performance across diverse benchmarks. This work offers a principled, extensible foundation for the development of personalization systems.

6 Acknowledgments

We sincerely thank all the reviewers for their encouraging and constructive feedback. This work was supported by the UKRI Future Leaders Fellowship under Grant MR/S017062/1 and MR/X011135/1; in part by NSFC under Grant 62376056 and 62076056; in part by the Royal Society Faraday Discovery Fellowship (FDF/S2/251014), BBSRC Transformative Research Technologies (UKRI1875), Royal Society International Exchanges Award (IES/R3/243136), Kan Tong Po Fellowship (KTP/R1/231017); and the Amazon Research Award and Alan Turing Fellowship.

References

Abbasnejad, E.; Sanner, S.; Bonilla, E. V.; and Poupart, P. 2013. Learning Community-Based Preferences via Dirichlet Process Mixtures of Gaussian Processes. In *IJCAI 2013, Proceedings of the 23rd International Joint Conference on Artificial Intelligence, Beijing, China, August 3-9, 2013*, 1213–1219. IJCAI/AAAI.

Austin, D. E.; Korikov, A.; Toroghi, A.; and Sanner, S. 2024. Bayesian Optimization with LLM-Based Acquisition Functions for Natural Language Preference Elicitation. In *Proceedings of the 18th ACM Conference on Recommender Systems, RecSys 2024, Bari, Italy, October 14-18, 2024*, 74–83.

Azar, M. G.; Guo, Z. D.; Piot, B.; Munos, R.; Rowland, M.; Valko, M.; and Calandriello, D. 2024. A General Theoretical Paradigm to Understand Learning from Human Preferences. In *International Conference on Artificial Intelligence and Statistics*, volume 238, 4447–4455. PMLR.

Bai, Y.; Jones, A.; Ndousse, K.; Askell, A.; Chen, A.; Das-Sarma, N.; Drain, D.; Fort, S.; Ganguli, D.; and et al., T. H. 2022. Training a Helpful and Harmless Assistant with Reinforcement Learning from Human Feedback. *CoRR*, abs/2204.05862.

Bengs, V.; Saha, A.; and Hüllermeier, E. 2022. Stochastic Contextual Dueling Bandits under Linear Stochastic Transitivity Models. In *International Conference on Machine Learning*, volume 162 of *Proceedings of Machine Learning Research*, 1764–1786.

Bradley, R. A.; and Terry, M. E. 1952. Rank Analysis of Incomplete Block Designs: I. The Method of Paired Comparisons. *Biometrika*, 39(3/4): 324–345.

Cohen, L.; Schmidt-Kraepelin, U.; and Mansour, Y. 2021. Dueling Bandits with Team Comparisons. In *Advances in Neural Information Processing Systems 34: Annual Conference on Neural Information Processing Systems 2021*, 20633–20644.

Deb, K.; Thiele, L.; Laumanns, M.; and Zitzler, E. 2005. Scalable Test Problems for Evolutionary Multiobjective Optimization. In *Evolutionary Multiobjective Optimization, Advanced Information and Knowledge Processing*, 105–145. Springer.

Di, Q.; Jin, T.; Wu, Y.; Zhao, H.; Farnoud, F.; and Gu, Q. 2024. Variance-aware Regret Bounds for Stochastic Contextual Dueling Bandits. In *The Twelfth International Conference on Learning Representations*.

Ding, B.; Qin, C.; Zhao, R.; Luo, T.; Li, X.; Chen, G.; Xia, W.; Hu, J.; Luu, A. T.; and Joty, S. 2024. Data Augmentation using LLMs: Data Perspectives, Learning Paradigms and Challenges. In *Findings of the Association for Computational Linguistics, ACL 2024*, 1679–1705.

Dudík, M.; Hofmann, K.; Schapire, R. E.; Slivkins, A.; and Zoghi, M. 2015. Contextual Dueling Bandits. In *Proceedings of The 28th Conference on Learning Theory, COLT 2015*, volume 40 of *JMLR Workshop and Conference Proceedings*, 563–587.

Dwaracherla, V.; Asghari, S. M.; Hao, B.; and Roy, B. V. 2024. Efficient Exploration for LLMs. In *Forty-first International Conference on Machine Learning, ICML 2024, Vienna, Austria, July 21-27, 2024*.

Ghazimatin, A.; Pramanik, S.; Roy, R. S.; and Weikum, G. 2021. ELIXIR: Learning from User Feedback on Explanations to Improve Recommender Models. In *WWW '21: The Web Conference 2021*, 3850–3860. ACM / IW3C2.

González, J.; Dai, Z.; Damianou, A.; and Lawrence, N. D. 2017. Preferential Bayesian Optimization. In *Proceedings of the 34th International Conference on Machine Learning*, volume 70 of *Proceedings of Machine Learning Research*, 1282–1291. PMLR.

Heckel, R.; Shah, N. B.; Ramchandran, K.; and Wainwright, M. J. 2016. Active ranking from pairwise comparisons and when parametric assumptions do not help. *The Annals of Statistics*.

Huang, T.; Wang, S.; and Li, K. 2024. Direct Preference-Based Evolutionary Multi-Objective Optimization with Dueling Bandits. In *The Thirty-eighth Annual Conference on Neural Information Processing Systems*.

Jamieson, K. G.; Katariya, S.; Deshpande, A.; and Nowak, R. D. 2015. Sparse Dueling Bandits. In *Proceedings of the Eighteenth International Conference on Artificial Intelligence and Statistics, AISTATS 2015, San Diego, California, USA, May 9-12, 2015*, volume 38 of *JMLR Workshop and Conference Proceedings*. JMLR.org.

Jedor, M.; Perchet, V.; and Louëdec, J. 2019. Categorized Bandits. In *Advances in Neural Information Processing Systems 32: Annual Conference on Neural Information Processing Systems 2019*, 14399–14409.

Kamishima, T.; and Akaho, S. 2010. Nantonac collaborative filtering: A model-based approach. In *Proceedings of the 2010 ACM Conference on Recommender Systems, RecSys 2010, Barcelona, Spain, September 26-30, 2010*, 273–276. ACM.

Lattimore, T.; and Szepesvári, C. 2020. *Bandit Algorithms*. Cambridge University Press.

Li, C.; Markov, I.; de Rijke, M.; and Zoghi, M. 2020. MergeDTS: A Method for Effective Large-Scale Online Ranker Evaluation. *ACM Trans. Inf. Syst.*, 38(4): 40:1–40:28.

Li, X.; Zhao, H.; and Gu, Q. 2024. Feel-Good Thompson Sampling for Contextual Dueling Bandits. In *Forty-first International Conference on Machine Learning, ICML 2024, Vienna, Austria, July 21-27, 2024*.

Lin, X.; Dai, Z.; Verma, A.; Ng, S.-K.; Jaillet, P.; and Low, B. K. H. 2024. Prompt Optimization with Human Feedback. In *ICML 2024 Workshop on Models of Human Feedback for AI Alignment*.

Mahalanobis; and (1936), P. 2018. On the Generalised Distance in Statistics. *Sankhya A*, 80: 1 – 7.

Munos, R.; Valko, M.; Calandriello, D.; Azar, M. G.; Rowland, M.; Guo, Z. D.; Tang, Y.; Geist, M.; Mesnard, T.; and Côme Fiegel, e. a. 2024. Nash Learning from Human Feedback. In *Forty-first International Conference on Machine Learning, ICML 2024, Vienna, Austria, July 21-27, 2024*.

Pan, S.; Luo, L.; Wang, Y.; Chen, C.; Wang, J.; and Wu, X. 2024. Unifying Large Language Models and Knowledge Graphs: A Roadmap. *IEEE Trans. Knowl. Data Eng.*, 36(7): 3580–3599.

Rafailov, R.; Sharma, A.; Mitchell, E.; Manning, C. D.; Ermon, S.; and Finn, C. 2023. Direct Preference Optimization: Your Language Model is Secretly a Reward Model. In *Advances in Neural Information Processing Systems 36: Annual Conference on Neural Information Processing Systems 2023, NeurIPS 2023, New Orleans, LA, USA, December 10 - 16, 2023*.

Razin, N.; Wang, Z.; Strauss, H.; Wei, S.; Lee, J. D.; and Arora, S. 2025. What Makes a Reward Model a Good Teacher? An Optimization Perspective. *CoRR*, abs/2503.15477.

Saha, A. 2021. Optimal Algorithms for Stochastic Contextual Preference Bandits. In *Advances in Neural Information Processing Systems 34: Annual Conference on Neural Information Processing Systems 2021*, 30050–30062.

Saha, A.; and Gaillard, P. 2022. Versatile Dueling Bandits: Best-of-both World Analyses for Learning from Relative Preferences. In *International Conference on Machine Learning*, volume 162 of *Proceedings of Machine Learning Research*, 19011–19026.

Slivkins, A. 2014. Contextual bandits with similarity information. *J. Mach. Learn. Res.*, 15(1): 2533–2568.

Song, K.; Tan, X.; Qin, T.; Lu, J.; and Liu, T. 2020. MPNet: Masked and Permuted Pre-training for Language Understanding. In *Advances in Neural Information Processing Systems*.

Srinivas, N.; Krause, A.; Kakade, S. M.; and Seeger, M. W. 2010. Gaussian Process Optimization in the Bandit Setting: No Regret and Experimental Design. In *Proceedings of the 27th International Conference on Machine Learning (ICML-10), June 21-24, 2010, Haifa, Israel*, 1015–1022. Omnipress.

Sui, Y.; Zhuang, V.; Burdick, J. W.; and Yue, Y. 2017. Multi-dueling Bandits with Dependent Arms. In *Proceedings of the Thirty-Third Conference on Uncertainty in Artificial Intelligence, UAI 2017, Sydney, Australia, August 11-15, 2017*.

Sun, H.; Pouplin, T.; Astorga, N.; Liu, T.; and van der Schaar, M. 2024. Improving LLM Generation with Inverse and Forward Alignment: Reward Modeling, Prompting, Fine-Tuning, and Inference-Time Optimization. In *The First Workshop on System-2 Reasoning at Scale, NeurIPS’24*.

Urvoy, T.; Clerot, F.; Féraud, R.; and Naamane, S. 2013. Generic exploration and K-armed voting bandits. In *ICML’13: Proc. of the 30th International Conference on Machine Learning*, 91–99. PMLR.

Verma, A.; Dai, Z.; Lin, X.; Jaillet, P.; and Low, B. K. H. 2025. Neural Dueling Bandits: Preference-Based Optimization with Human Feedback. In *The Twelfth International Conference on Learning Representations, ICLR 2025*. OpenReview.net.

Wang, S.; and Li, K. 2024. Constrained Bayesian Optimization under Partial Observations: Balanced Improvements and Provable Convergence. In *Thirty-Eighth AAAI Conference on Artificial Intelligence 2024*, 15607–15615. AAAI Press.

Wu, H.; and Liu, X. 2016. Double Thompson Sampling for Dueling Bandits. In *Advances in Neural Information Processing Systems 29: Annual Conference on Neural Information Processing Systems 2016*, 649–657.

Xiao, T.; Ge, Z.; Sanghavi, S.; Wang, T.; Katz-Samuels, J.; Versage, M.; Cui, Q.; and Chilimbi, T. 2025. InfoPO: On Mutual Information Maximization for Large Language Model Alignment. In *Proceedings of the 2025 Conference of the North American Chapter of the Association for Computational Linguistics*. Association for Computational Linguistics.

Xiong, W.; Dong, H.; Ye, C.; Wang, Z.; Zhong, H.; Ji, H.; Jiang, N.; and Zhang, T. 2024. Iterative Preference Learning from Human Feedback: Bridging Theory and Practice for RLHF under KL-constraint. In *Forty-first International Conference on Machine Learning, ICML 2024, Vienna, Austria, July 21-27, 2024*.

Yang, X.; Lu, J.; and Yu, E. 2025. Walking the Tightrope: Disentangling Beneficial and Detrimental Drifts in Non-Stationary Custom-Tuning. In *The Thirty-ninth Annual Conference on Neural Information Processing Systems*.

Yi, B.; Kang, Y.; and Li, Y. 2024. Biased Dueling Bandits with Stochastic Delayed Feedback. *Transactions on Machine Learning Research*.

Yu, E.; Lu, J.; Yang, X.; Zhang, G.; and Fang, Z. 2025. Learning Robust Spectral Dynamics for Temporal Domain Generalization. In *The Thirty-ninth Annual Conference on Neural Information Processing Systems*.

Yue, Y.; Broder, J.; Kleinberg, R.; and Joachims, T. 2012. The K-armed dueling bandits problem. *J. Comput. Syst. Sci.*, 78(5): 1538–1556.

Zhao, C.; Yu, T.; Xie, Z.; and Li, S. 2022. Knowledge-aware Conversational Preference Elicitation with Bandit Feedback. In *WWW ’22: The ACM Web Conference 2022, Virtual Event, Lyon, France, April 25 - 29, 2022*, 483–492. ACM.

Zoghi, M.; Karnin, Z. S.; Whiteson, S.; and de Rijke, M. 2015. Copeland Dueling Bandits. In *Advances in Neural Information Processing Systems 28: Annual Conference on Neural Information Processing Systems 2015, December 7-12, 2015, Montreal, Quebec, Canada*, 307–315.

Zoghi, M.; Whiteson, S.; Munos, R.; and de Rijke, M. 2014. Relative Upper Confidence Bound for the K-Armed Dueling Bandit Problem. In *Proceedings of the 31th International Conference on Machine Learning, ICML 2014, Beijing, China, 21-26 June 2014*, volume 32, 10–18.

7 Related Work

7.1 Dueling Bandits

Dueling bandits (DB), which leverage duel feedback for online decision-making, were first introduced by (Yue et al. 2012) and have since become a core paradigm in IPE. Depending on the availability of additional information, DB algorithms are generally categorized into two classes.

Stochastic Dueling Bandits In stochastic DB, each pair of arms is associated with an unknown winning probability. Early work relied on strong stochastic transitivity assumptions (Yue et al. 2012), while subsequent research has shifted toward more general definition of winners. The Condorcet winner, as used in our work, was introduced in (Urvoy et al. 2013). Building on this, the RUCB algorithm was proposed in (Zoghi et al. 2014), establishing insightful theoretical foundations for the DB framework. Another important type of winner is the Copeland winner (Zoghi et al. 2015), which generalizes the Condorcet assumption and underpins the analysis of the DTS algorithm (Wu and Liu 2016). The Borda winner, as introduced in (Jamieson et al. 2015), enables a theoretically efficient DB algorithm under sparse feedback. Different from our method, it requires additional structural assumptions on the preference matrix to ensure sample efficiency (Jamieson et al. 2015). In this work, we adopt the Copeland winner assumption due to its compatibility with UCB-based decision-making and its widespread use in prior studies (see the regret equivalence in (Saha 2021)). Extensions of stochastic DB algorithms to more complex scenarios including adversarial preferences (Saha and Gaillard 2022) and delayed feedback (Yi, Kang, and Li 2024) have also been proposed, offering potential robustness verification of our methods.

Contextual Dueling Bandits In our work, context provides side information that encodes similarity or structural relationships among candidates. This notion aligns with broader research in preference optimization, including reinforcement learning with human feedback (Rafailov et al. 2023) and preferential optimization (González et al. 2017). A different notion of context is considered in (Dudík et al. 2015), where the context is chosen by nature and reflects the dynamic structure of the preference matrix across time. To leverage the context-based side information, existing methods typically fall into three categories:

- **Structured reward estimation.** By predefining a shared reward structure originating from linear bandits (Lattimore and Szepesvári 2020), the objective in IPE shifts from identifying the most preferred candidate to estimating the underlying utility function. Algorithms and variants that generalize to subset-wise comparisons were proposed in (Saha 2021). Following on, more flexible parametric models are studied in (Bengs, Saha, and Hüllermeier 2022; Di et al. 2024). Most recently, to mitigate the risks of model misspecification, neural estimator has been introduced in (Verma et al. 2025). Most of these methods adopt deterministic strategies, while random strategy such as Thompson sampling has been recently integrated as a promising alternatives for linear contextual DB (Li, Zhao, and Gu 2024). A key limitation of this line of work is the inability to quantify the impact of misleading model assumptions. In contrast, our method explicitly captures both the potential benefits and risks of feedback augmentation, without requiring a predefined parametric structure.
- **Candidate partitioning.** To reduce search and sample complexity, early work leveraged contextual similarity to partition candidates into subsets (Slivkins 2014). This transforms the objective from identifying the single most preferred candidate to locating coarse-grained regions of interest (Huang, Wang, and Li 2024). In DB literature, partitioning strategies include clustering (Huang, Wang, and Li 2024), merging (Li et al. 2020), and grouping (Cohen, Schmidt-Kraepelin, and Mansour 2021). These approaches often fail to capture fine-grained preferences or more complex contextual relationships. An exception is MergeDTS (Li et al. 2020), whose sample complexity remains comparable to non-merged alternatives. Our framework generalizes partition-based DB methods as a special case and retains the ability to identify the best single candidate, enabling finer preference resolution when needed.
- **Similarity and dependency.** There are limited studies on similarity functions (Lattimore and Szepesvári 2020) and dependent arms (Sui et al. 2017). As suggested by our results, similarity alone is often insufficient to fully capture the relational structure among candidates. Motivated by this limitation, our approach shifts focus from raw similarity to more expressive notions of dependency, which we estimate through annotations derived from richer forms of human feedback. This allows us to capture more nuanced, asymmetric, and context-sensitive relationships, ultimately enabling more effective augmentation of human preferences.

7.2 Augmentation and Richer Forms of Human Feedback

In addition to the DB framework, several algorithms for IPE and general preference optimization have explored the integration of richer forms of feedback through augmentation. When candidate items are associated with feature-level keys, both the items and their attributes can serve as contextual information. The relationships between them can be characterized using structured representations such as knowledge graphs (Zhao et al. 2022). This operation enables querying formats beyond pairwise comparisons, allowing for feature-level preference elicitation (Austin et al. 2024). Similar strategies have been adopted in the context of LLMs, where human explanations and rationales offer valuable guidance during fine-tuning (Ghazimatin et al. 2021). In language processing, natural language inference and LLMs have also been employed for relation augmentation and annotation (Ding et al. 2024). Graph-based representations, as supported by recent work and our findings, have the potential to offer a strong foundation for both structured feedback and preference optimization in IPE (Pan et al. 2024).

8 Details of Proposed Algorithms

We integrate the augmented confidence bounds into two canonical DB algorithms: RUCB and DTS. They belong to different types of DB strategies, the RUCB is deterministic, while the DTS is stochastic. Different types of strategies apply to different IPE scenarios, for instance, DTS is observed more efficient for response optimization in LLM exploration (Dwaracherla et al. 2024).

The full pseudo-code of `IPEA-RUCB` is provided in Algorithm 2. Its core selection strategy follows the original RUCB algorithm, with additional components for dependency extraction and feedback augmentation. The overall structure of `IPEA-DTS` is analogous to that of `IPEA-RUCB`, differing primarily in its use of Thompson sampling with majority voting for arm selection. For completeness, we refer readers to the original DTS paper (Wu and Liu 2016) and our implementation; we omit the full pseudo-code of `IPEA-DTS` here for brevity.

Algorithm 2: Pseudo-code of `IPEA-RUCB`

```

1: Input: Candidate number  $K$ , context set  $\mathcal{X}$ ,  $\alpha > 0$ , similarity threshold  $\tau$ , IPE budget  $T$ 
2: Init: Winning matrix  $\mathbf{B} = [0]_{K \times K}$ , similarity-based undirected graph  $\mathcal{G}(\mathcal{X}, K)$  with edges determined by  $\tau$ , dependency
   dictionary  $W = [0]$ , candidate set  $\mathcal{B} = \emptyset$ ,  $t = 0$ 
3: repeat
4:   / *** Implementation of AugConfidanceBound ***
5:   for  $i, j \in \mathcal{A}, i \neq j$  do
6:     Get tuples of related observations  $\mathcal{T}_{n_{i,j}^r} \leftarrow (W, \mathcal{G}).get(i, j)$ ,  $n_{i,j}^r \leftarrow 0$ ,  $n_w^r \leftarrow 0$ ,  $X_{i,j} \leftarrow 0$ 
7:     for  $(a_m, a_n, w_{i,j}^{m,n}) \in \mathcal{T}_{n_{i,j}^r}$  do
8:        $n_{i,j}^r \leftarrow n_{i,j}^r + b_{m,n} + b_{n,m}$ ,  $n_w^r \leftarrow n_w^r + w_{i,j}^{m,n} * (b_{m,n} + b_{n,m})$ ,  $X_{i,j} \leftarrow X_{i,j} + b_{m,n}$ 
9:     end for
10:     $\hat{p}_{i,j} = \frac{b_{i,j} + X_{i,j}}{b_{i,j} + b_{j,i} + n_w^r}$ ,  $\hat{u}_{i,j} = \hat{p}_{i,j} + \sqrt{\frac{\alpha(b_{i,j} + b_{j,i} + n_{i,j}^r) \log t}{(b_{i,j} + b_{j,i} + n_w^r)^2}}$  {equation (3),  $\frac{x}{0} := 1, \forall x$ }
11:   end for
12:   / *** Implementation of DuelingBanditAlgo *** / {RUCB algorithm in (Zoghi et al. 2014)}
13:    $\mathcal{C} \leftarrow \{a_c | \forall j : \hat{u}_{c,j} \geq 0.5\}$ , if  $\mathcal{C} = \emptyset$ : then  $\mathcal{C} \leftarrow \{a_c | c = \text{Random}(K)\}$ ,  $\mathcal{B} \leftarrow \mathcal{B} \cap \mathcal{C}$ 
14:   Sample  $a_c$  from  $\mathcal{C}$  according to distribution: if  $a_c \in \mathcal{B}$ :  $p(a_c) = 0.5$ , else  $p(a_c) = \frac{1}{2|\mathcal{B}| - |\mathcal{C} \setminus \mathcal{B}|}$ 
15:   Obtain  $a_d$  where  $d \leftarrow \arg \max_j \hat{u}_{j,c}$ , ties broken randomly with  $d \neq c$ 
16:   Query user preference on  $(a_c, a_d)$ , with  $X \sim \text{Bernoulli}(p_{c,d})$ 
17:   if  $X = 1$ :  $b_{c,d} \leftarrow b_{c,d} + 1$  else  $b_{d,c} \leftarrow b_{d,c} + 1$ 
18:   / *** Implementation of DependencyExtract & FeedbackAug ***
19:   Obtain related pairs  $\{(a_m, a_n)\}$  from similarity graph  $\mathcal{G}$  through connectivity
20:   Get additional annotations  $w_{c,d}^{m,n}$  from user / LLMs
21:   Update  $(W, \mathcal{G}).append((c, d) : (m, n, w_{c,d}^{m,n}))$  {add related observations with dependency}
22:   Get richer forms of feedback  $F(a_c, a_d)$  and update  $\mathcal{G}$  {this step is optional}
23:    $t \leftarrow t + 1$ 
24: until  $t > T$ 

```

9 Experimental Setup and Implementation Details

9.1 Benchmark Problems

Sushi Dataset Details The Sushi dataset¹ collects full rankings over 10 popular types of sushi from Japanese customers. It contains 5,000 customer orders, along with item features and user demographic information. To construct the preference matrix, we traverse all orders and, for each pair of sushi items, count the number of times the higher-ranked item wins over the lower-ranked item. The resulting counts are then normalized by the total number of comparisons for each sushi pair. To incorporate contextual information, we leverage the item features listed in Table 1.

Among all sushi types, toro (fatty tuna) is the most preferred item, identified as the Condorcet winner in the preference matrix, with the feature vector: [8, toro, 1, 0, 1, 0.55, 2.06, 4.49, 0.80]. For our analysis, we discard the ID and Name features and normalize numerical features (Heaviness Taste, Eating frequency, Price, Selling Frequency) consistently across all algorithms. Figure 8 presents both the 2-dimensional multidimensional scaling (MDS) projection and the hierarchical clustering dendrogram of sushi items based on their features. The figure suggests that sushi items do not clearly separate into distinct subsets, implying that partition-based methods might yield suboptimal performance in this scenario.

¹<https://www.kamishima.net/sushi/>

Table 1: Item features for the Sushi dataset.

| Feature | Type | Value Space |
|-------------------|-------------|---------------------------------------|
| Item ID | Categorical | 1-10 |
| Name | Categorical | Roman alphabets of sushi type |
| Style | Binary | 0 (maki), 1 (otherwise) |
| Major Group | Binary | 0 (seafood), 1 (otherwise) |
| Minor Group | Categorical | 0 (blue skinned fish)-11 (vegetables) |
| Heaviness Taste | Numerical | [0-4], 0: heavy |
| Eating frequency | Numerical | [0-3], 3: most frequently |
| Price | Numerical | - |
| Selling Frequency | Numerical | [0-1], 1: most frequently |

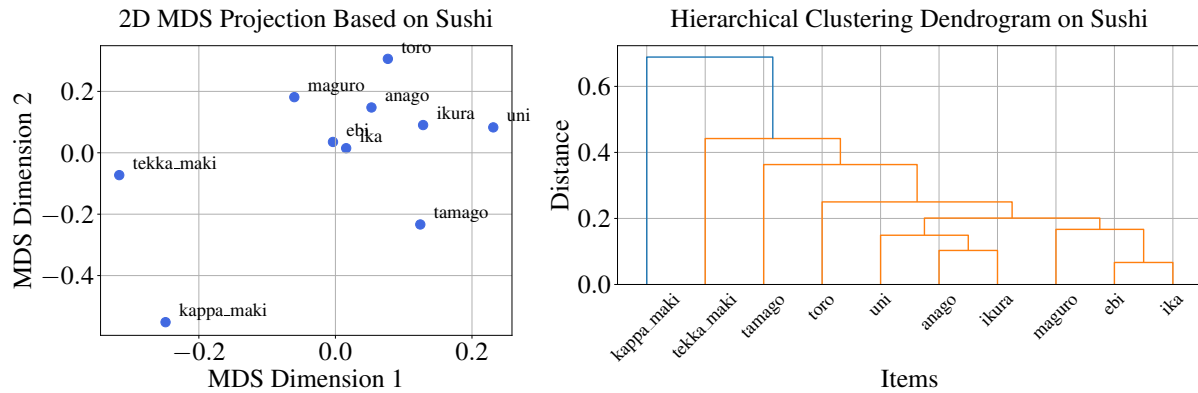


Figure 8: Hierarchical clustering dendrogram of Sushi items using Gower distance. Vertical distances indicate dissimilarity; branches closer together denote similar items.

Car Preference Dataset Details The Car Preference dataset² collects full ranking over 10 types of cars from 60 American users in Amazon Mechanical Turk. We conduct the same operation as the Sushi experiment to obtain the preference matrix. The item features are listed in Table 2.

Table 2: Item features for the Car Preference dataset.

| Feature | Type | Value Space |
|-----------------|-------------|------------------------------|
| Item ID | Categorical | 1-10 |
| Body Type | Binary | 1 (Sedan), 2 (SUV) |
| Transmission | Binary | 1 (Manual), 2 (Automatic) |
| Engine Capacity | Categorical | 2.5L, 3.5L, 4.5L, 5.5L, 6.2L |
| Fuel Consumed | Binary | 1 (Hybrid), 2 (Non-Hybrid) |

Among all car types, the sixth car is the most preferred item, identified as the Condorcet winner in the preference matrix, with the feature vector: [2, 2, 3.5L, 1]. Figure 9 presents both the 2-dimensional multidimensional scaling (MDS) projection and the hierarchical clustering dendrogram of sushi items based on their features. The figure suggests that car items may be clearly separated into distinct subsets (4 subsets and two single items 9 and 10).

Synthetic DTLZ The synthetic DTLZ problems are commonly used for benchmarking in research of multi-objective optimization (Huang, Wang, and Li 2024). We select two DTLZ problems (DTLZ2 and DTLZ7) with different Pareto fronts as visualized in Figure 10. Note that DTLZ 1-4 share the same characteristics in Pareto fronts, while DTLZ 5 and DTLZ 6 is much simpler than other problems in DTLZ family in terms of preference optimization.

We use the *a posteriori* method of multi-objective optimization to focus on the IPE task. We sample 100 non-dominant solutions in objective space using NSGA-II, one of the most prestigious evolutionary-based algorithm. Following the settings in (Huang, Wang, and Li 2024), we randomly select one sample as the best winner, denoted as \vec{x}_* . Then, we construct the

²<https://ehsanabb.github.io/CarPreferences.html>

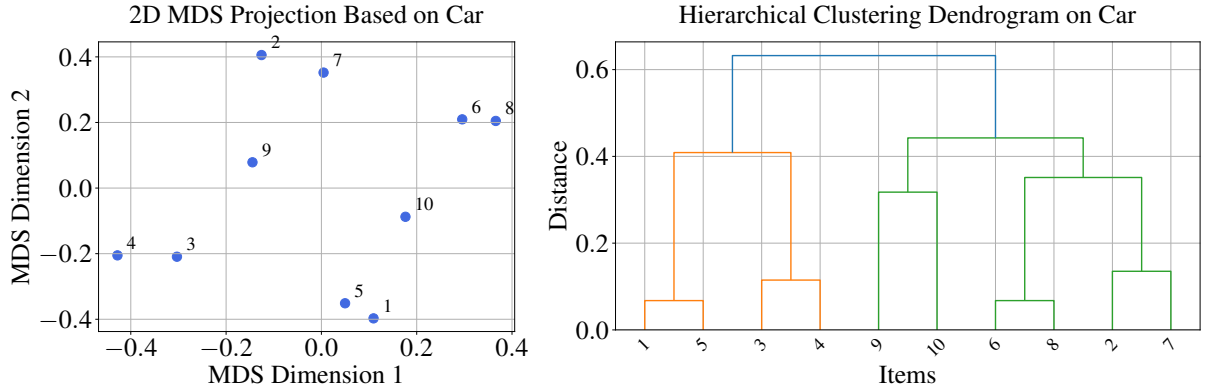


Figure 9: Hierarchical clustering dendrogram of Car items using Gower distance.

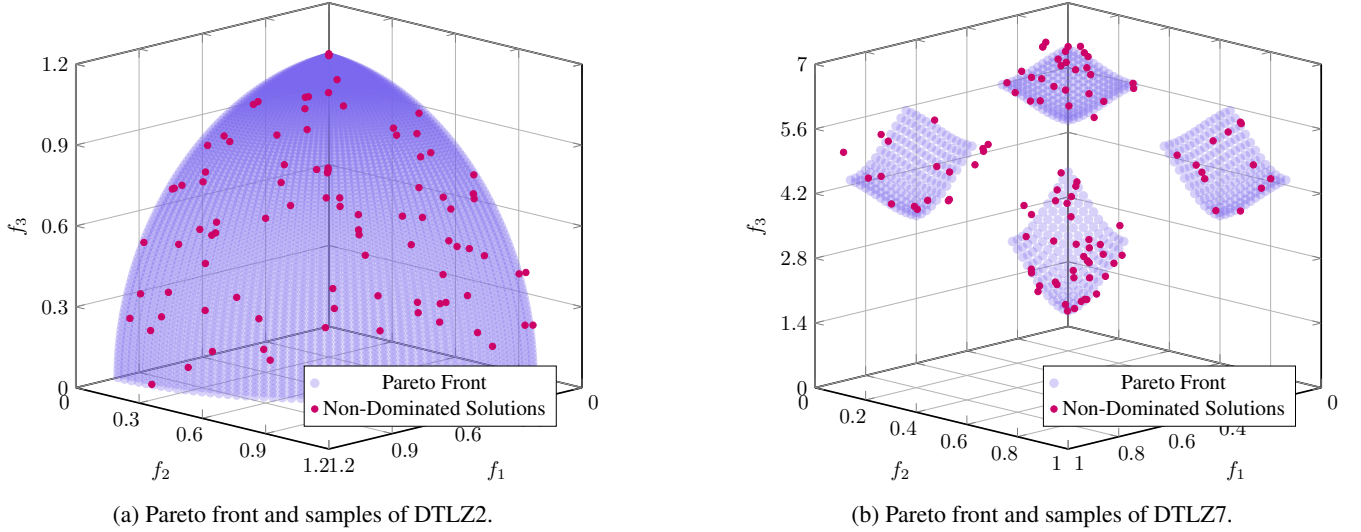


Figure 10: DTLZ Pareto front with 100 samples in 3-dimensional objective space.

preference matrix by

$$p_{i,j} = \text{sigmoid} \left(\frac{u_i - u_j}{\tau} \right), \quad u_i = \mathcal{N}(\vec{x}_i | \vec{x}_*, \sigma \mathbf{I}), \quad i, j \in \{1, 2, \dots, 100\}. \quad (8)$$

Here, \vec{x}_i denotes the decision variable of a sampled solution. We set the preference noise threshold to $\tau = 0.2$ to generate clearer pairwise preferences. The DTLZ problem involves a 10-dimensional decision variable and a 3-dimensional objective vector. We concatenate these two components to form a 13-D feature vector for each solution. This unified representation is used by the parametric DB algorithms and serves as the input for similarity computation within our framework.

LLM Exploration We follow the official codebase³ provided by the authors of (Lin et al. 2024). The prompt optimization task can be formulated as a contextual DB problem. Specifically, given a prompt x_i , instead of generating two responses randomly for preference optimization, one can generate a large pool of candidate responses and actively select the one mostly aligned with human preferences. This process is also referred to as active exploration in the literature (Dwaracherla et al. 2024). As depicted in Figure 11, this task fits naturally within the contextual DB setting (Lattimore and Szepesvári 2020), where each prompt (context) is associated with a preference matrix, and the objective is to identify the optimal arm given the current context.

We randomly sample 5 prompts from the Anthropic Helpfulness and Harmlessness datasets as different contexts, and generate 20 responses for each prompt using GPT-3.5-turbo. To mimic human preferences, we leverage a fine-tuned reward model based on GPT-2 trained on the same datasets⁴ as the reward function f . Pairwise winning probabilities are computed using the

³<https://github.com/xqlin98/APOHF>

⁴https://huggingface.co/Ray2333/gpt2-large-helpful-reward_model

BT model. Note that for a given prompt, only responses from the same pool are valid for comparisons, while inter-prompt comparisons are meaningless for IPE. Consequently, standard DB algorithms without explicit mechanisms for dealing with inter-prompt contextual information (Lin et al. 2024; Verma et al. 2025) must maintain 5 separate winning matrices or parametric models and select the candidates based on current prompt/context. Our algorithms face the same difficulty, but are able to go further: they leverage augmented feedback not only from responses within the same prompt/context, but also from other prompts, provided strong contextual similarity and dependency can be established. Since these augmented observations originate from different candidate pools, we treat them as a distinct form of human feedback.

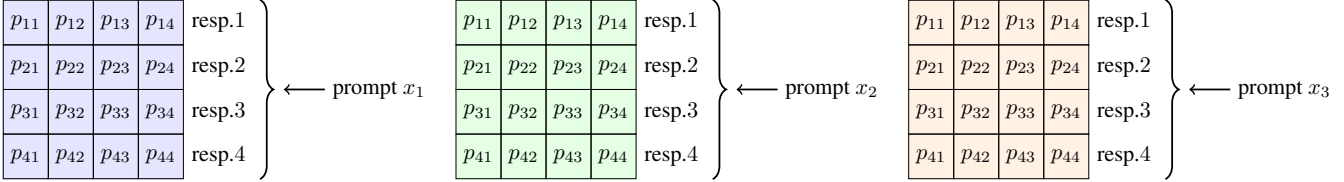


Figure 11: Illustration of preference matrices in response optimization. This represents a contextual dueling bandit (DB) setting, where each context corresponds to a different prompt, and is associated with a distinct pool of response candidates and its own preference matrix.

9.2 Algorithmic Details and Configurations

Peer Algorithms We use the official implementation of VACDB⁵, which also include the implementation of MaxInP and COLSTM. We keep the default setting of the three algorithms. We implement RUCB and DTS in Python according to descriptions in literature.

For mixed-valued feature spaces (e.g., Sushi and Car Preference datasets), we compute pairwise similarity using the default Gower distance. For datasets with purely numerical features (e.g., DTLZ and LLM Exploration), we apply Euclidean distance after normalization with `MinMaxScaler` from `sklearn`. The similarity threshold for feedback augmentation is set to 0.85 across all experiments. For LLM-based annotation, we set the temperature as 0.9 to encourage variability. We use a fixed confidence parameter of $\alpha = 0.1$ for RUCB, DTS, and our proposed algorithms. The sensitivity of our method to different α values is further analyzed in Section 10.2.

Experimental Configurations we run all experiments on a MacBook Pro equipped with an Apple M3 Pro chip and 36 GB of RAM. For each benchmark, every algorithm is executed with 10 different random seeds. The regret trajectories reported in all figures represent the mean regret, with shaded regions denoting ± 0.5 standard deviation. All implementations are written in Python, and major dependencies (e.g., `numpy`, `scikit-learn`, `gower`, and `networkx`) are publicly available. To speed up the experiments, we pre-process all benchmarks into a unified data format, including the preference matrix, similarity graph, and dependency dictionary.

9.3 Prompt Design for Dependency Annotation

We use the following prompts for LLM annotator (GPT-3.5-Turbo) to reason conditional dependency.

Prompt for Sushi Recommendation

You are assisting in eliciting user preferences in the context of sushi recommendation.

Here are four sushi types with their descriptions:

- Item A: ebi, style not maki, major group seafood, minor group blue-skinned fish, ...
- Item B: anago, style not maki, major group seafood, minor group red meat fish, ...
- Item C: ebi, style not maki, major group seafood, minor group blue-skinned fish, ...
- Item D: ikura, style not maki, major group seafood, minor group squid or octopus, ...

Assume the following: The user has shown a strong preference for Item A over Item B.
You should consider both the features and your experience.

Please reason briefly about how this affects the likelihood of preferring Item C over Item D, and then on a separate line, provide only the numeric score from 0 to 1.

⁵<https://github.com/uclaml/VACDB>

Accordingly, one piece of the response from GPT is:

LLM Response to Sushi Preference Dependency (GPT 3.5 Turbo)

Given that the user has a strong preference for Item A over Item B, it is likely that they would also prefer Item C over Item D since both items share similar characteristics with Item A in terms of the type of seafood (ebi) and eating frequency. Additionally, both Item A and Item C have a higher selling frequency compared to Item B and D, indicating they are more popular choices among consumers.

Numeric score: 0.8

In Car recommendation, we use the following prompt structure:

Prompt for Car Recommendation

You are assisting in eliciting user preferences in the context of car recommendation.

Here are four car types with their descriptions:

- Item A: body type SUV, transmission Manual, engine capacity 2.5, ...
- Item B: body type Sedan, transmission Automatic, engine capacity 3.5, ...
- Item C: body type SUV, transmission Manual, engine capacity 3.5, ...
- Item D: body type Sedan, transmission Automatic, engine capacity 3.5, ...

Assume the following: The user has shown a strong preference for Item A over Item B.

You should consider both the features and your experience. Please reason briefly about how this affects the likelihood of preferring Item C over Item D, and then on a separate line, provide the value of numeric score in [0, 1].

Accordingly, one piece of the response from GPT is:

LLM Response to Car Preference Dependency (GPT 3.5 Turbo)

Given that the user has a strong preference for Item A over Item B, it is likely that they value the body type (SUV) and transmission type (Manual) over engine capacity and fuel consumption. Therefore, it is possible that they may also prefer Item C over Item D, as it shares the same body type and transmission type as Item A.

Numeric score: 0.75

10 Experimental Results

10.1 Additional Results

Similarity Graph The similarity graph guides the algorithms to focus on the most informative candidate pairs, represented by the edges, which are likely to yield meaningful dependency information. The constructed graphs for each benchmark are visualized in Figure 12. The graph structures for Sushi and Car are consistent with the similarity analyses presented in Figures 8 and 9. Notably, the size of the resulting dependency dictionaries varies across benchmarks. This is particularly evident in the response optimization task, where only comparisons among responses under the same prompt are retained, imposing an additional structural constraint that is absent in the DTLZ problems.

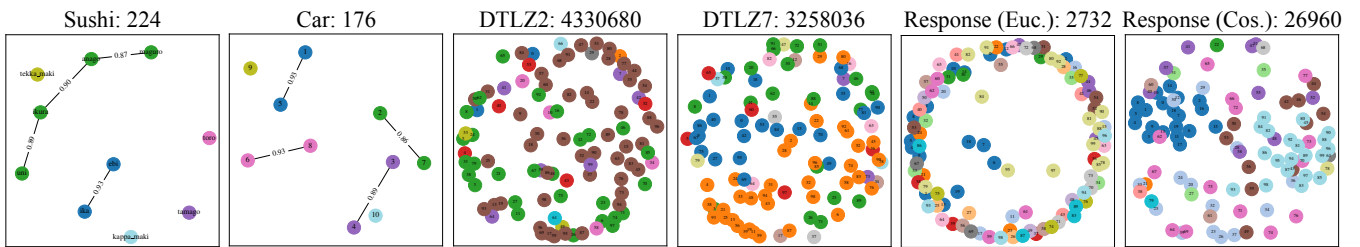


Figure 12: Similarity graph and total size of dependency dictionaries for each benchmark, under a similarity threshold of 0.85. In LLM response, we use both Euclidean and Cosine distances.

Multi-Objective Optimization The results on DTLZ2 problem are given in Figure 13. We also present numerical scores of each algorithm in Table 3, demonstrating a better trade-off of our algorithms between regret minimization and query diversity.

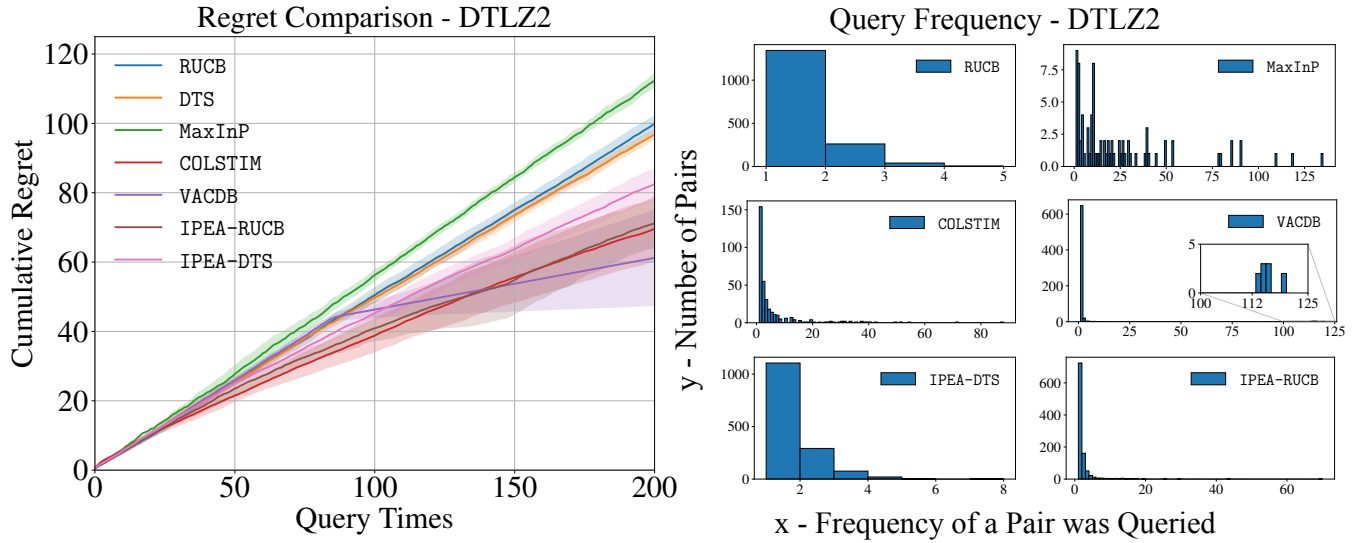


Figure 13: Regret and query frequency analysis on DTLZ2.

Table 3: Query Statistics Across Algorithms in DTLZ Benchmarks

| Exp. | Metric | RUCB | DTS | MaxInP | COLSTIM | VACDB | IPEA-RUCB | IPEA-DTS |
|-------|--------------------|-------|-------|--------|---------|-------|-----------|----------|
| DTLZ2 | Total Queries | 2000 | 2000 | 2000 | 2000 | 2000 | 2000 | 2000 |
| | Unique Pairs | 1651 | 1658 | 83 | 351 | 687 | 1020 | 1496 |
| | Entropy (bits) | 10.59 | 10.60 | 5.53 | 7.20 | 6.81 | 9.21 | 92.2% |
| | Normalized Entropy | 99.1% | 99.2% | 86.8% | 85.1% | 72.3% | 92.2% | 98.7% |
| DTLZ7 | Total Queries | 2000 | 2000 | 2000 | 2000 | 2000 | 2000 | 2000 |
| | Unique Pairs | 1650 | 1668 | 89 | 171 | 484 | 875 | 1568 |
| | Entropy (bits) | 10.59 | 10.62 | 5.71 | 5.95 | 4.10 | 9.27 | 10.49 |
| | Normalized Entropy | 99.1% | 99.2% | 88.2% | 80.2% | 46.0% | 94.8% | 98.9% |

10.2 Parameter Sensitivity

We study the sensitivity of the exploration parameter α in both IPEA-RUCB and IPEA-DTS. This parameter controls the degree of exploration: higher values of α encourage more exploratory behavior. To assess its effect on convergence, we choose the recommendation tasks using three representative values of α from the set $[0.1, 0.51, 0.8]$. The comparative results are presented in Figure 14.

Our findings suggest that the deterministic strategies, such as RUCB and IPEA-RUCB, are more sensitive to changes in α . This sensitivity reflects a potential weakness of deterministic strategies as they may be more susceptible to suboptimal parameter settings, in contrast to stochastic strategies (e.g., DTS and IPEA-DTS), as has been noted in (Wu and Liu 2016; Huang, Wang, and Li 2024; Dwaracherla et al. 2024). However, IPEA-RUCB consistently outperforms the behaviors of original RUCB, demonstrating the effectiveness of feedback augmentation.

In contrast, both DTS and IPEA-DTS exhibit minimal sensitivity to α , with stable performance across the tested range. Based on our experiments, a fixed setting of $\alpha = 0.1$ proves effective for IPEA-RUCB in most cases. For IPEA-DTS, $\alpha = 0.1$ is also recommended, though other values yield comparably strong performance.

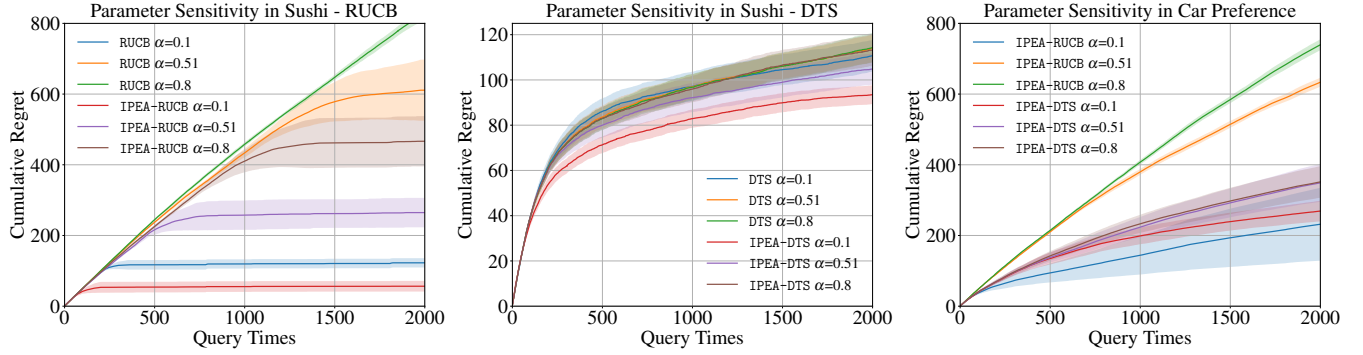


Figure 14: Regret trajectories for Sushi and Car Preference experiments under different values of α .

11 Theoretical Analysis

In this section, we present formal proofs and detailed derivations for our main theoretical results. We begin by introducing a general form of the Chernoff–Hoeffding inequality as a foundational lemma. Building on this, we prove Theorem 3.1, which establishes the concentration property under augmented feedback. We then derive the calibration threshold that characterizes when augmented feedback contributes positively to concentration. Subsequently, we analyze the total sample complexity for each pair under the IPEA–RUCB algorithm, supporting the claims stated in Theorem 3.2. Finally, we provide the proof of Theorem 3.3, which characterizes the regret bound within IPEA–RUCB.

Lemma 11.1 (Chernoff–Hoeffding inequality). *Suppose that random variables X_1, \dots, X_n are independent, $a_i \leq X_i \leq b_i$, and let $E[X_i] = \mu$. Then for any $\sigma > 0$, the following inequality holds:*

$$P\left(\left|\frac{1}{n} \sum_{i=1}^n X_i - \mu\right| \geq \sigma\right) \leq 2 \exp\left(-\frac{2n^2\sigma^2}{\sum_{i=1}^n (b_i - a_i)^2}\right). \quad (9)$$

This inequality applies to independent random variables that are not necessarily identically distributed, a property that is particularly useful for our theoretical analysis with augmented human feedback. In the context of dueling bandits, where the random variables are Bernoulli-distributed (i.e., $a_i = 0$ and $b_i = 1$ for $i = 1, \dots, n$), the inequality can be formulated as follows:

$$P\left(\frac{1}{n} \sum_{i=1}^n X_i \geq \mu + \sigma\right) \leq \exp(-2n\sigma^2), \quad P\left(\frac{1}{n} \sum_{i=1}^n X_i \leq \mu - \sigma\right) \leq \exp(-2n\sigma^2). \quad (10)$$

11.1 Concentration Property: Proof of Theorem 3.1

Proof. We follow the steps in (Zoghi et al. 2014) by first introducing the notation for the *good* event $\mathcal{E}_{i,j}(t)$, which denotes that at time t , the true preference probability satisfies $p_{i,j} \in [\hat{l}_{i,j}(t), \hat{u}_{i,j}(t)]$. Note that $\mathcal{E}_{i,i}(t)$ holds for all t and that $\mathcal{E}_{i,j}(t) = \mathcal{E}_{j,i}(t)$ for all $i, j \in \mathcal{A}$. Therefore, we focus without loss of generality on the case where $i > j$. We define $\tau_{i,j}^n$ as the time at which the n -th total observation for the pair (a_i, a_j) occurs. Here, the total observations include both direct comparisons between a_i and a_j , and related observations inferred from comparisons involving other arms. Another fact is that for $T' \in [\tau_{i,j}^n, \tau_{i,j}^{n+1}]$, if $\mathcal{E}_{i,j}(T')$ holds, then $\mathcal{E}_{i,j}(t)$ also holds for all $t \in [T', \tau_{i,j}^{n+1}]$. This is true because for $t \in [\tau_{i,j}^n, \tau_{i,j}^{n+1}]$, the uncertainty terms in $\hat{u}_{i,j}$ and $\hat{l}_{i,j}$ increase monotonically. Consequently, for any T' and all subsequent times $t > T'$, the probability of event $\mathcal{E}_{i,j}(t)$ occurring is expressed as follows:

$$P(\forall t \geq T', i, j, \mathcal{E}_{i,j}(t)) = P(\forall i > j, \mathcal{E}_{i,j}(T') \wedge \forall n \text{ s.t. } \tau_{i,j}^n > T', \mathcal{E}_{i,j}(\tau_{i,j}^n)). \quad (11)$$

Conversely, the *bad* event $\mathcal{B}_{i,j}(t)$, defined as the event that $p_{i,j} \notin [\hat{l}_{i,j}(t), \hat{u}_{i,j}(t)]$ at the t -th iteration, can be bounded by the following inequality, applying notions from equation (3):

$$\begin{aligned}
P(\exists t \geq T', i, j, \mathcal{B}_{i,j}(t)) &= 1 - P(\forall t \geq T', i, j, \mathcal{E}_{i,j}(t)) \\
&\leq \sum_{i < j} [P(\mathcal{B}_{i,j}(T')) + P(\exists n \text{ s.t. } \tau_{i,j}^n > T', \mathcal{B}_{i,j}(\tau_{i,j}^n))] \\
&\leq \sum_{i < j} \left[2 \sum_{n=0}^{T'} P\left(|p_{i,j} - \hat{p}_{i,j}(n)| > \frac{1}{\eta(n)} \sqrt{\frac{\alpha \ln T'}{n}}\right) \right. \\
&\quad \left. + \sum_{n=T'+1}^{\infty} P\left(|p_{i,j} - \hat{p}_{i,j}(n)| > \frac{1}{\eta(n)} \sqrt{\frac{\alpha \ln n}{n}}\right) \right]. \tag{12}
\end{aligned}$$

The final step of the above inequalities holds as proven in (Zoghi et al. 2014). For conciseness, we let $\hat{p}_{i,j}(n)$ denote the estimate of $p_{i,j}$ given n total observations. Similarly, we explicitly denote the dependency of η on n by writing it as $\eta(n)$.

On the other hand, given $n_{i,j}^d$ independent observations drawn from $\text{Bernoulli}(p_{i,j})$ and $n_{i,j}^r$ additional independent observations drawn from separate distributions $\text{Bernoulli}(w_{i,j}^k p_{i,j})$ for $k = 1, \dots, n_{i,j}^r$, the expectation of the combined observations can be expressed as follows:

$$\mu = \frac{n_{i,j}^d}{n_{i,j}} p_{i,j} + \frac{1}{n_{i,j}} \sum_{k=1}^{n_{i,j}^r} w_{i,j}^k p_{i,j} = \frac{1}{n_{i,j}} \left(n_{i,j}^d + \sum_{k=1}^{n_{i,j}^r} w_{i,j}^k \right) p_{i,j} := \eta p_{i,j}. \tag{13}$$

By applying the generalized Chernoff-Hoeffding inequality in equation (9), we have

$$P\left(\left|\frac{1}{n_{i,j}} \left(b_{i,j} + \sum_{k=1}^{n_{i,j}^r} X_{i,j}^k\right) - \eta p_{i,j}\right| \geq \sigma\right) \leq 2 \exp(-2n_{i,j}\sigma^2), \tag{14}$$

for any $\sigma > 0$. Dividing both sides of the inequality inside the probability by η , we obtain

$$P(|\hat{p}_{i,j} - p_{i,j}| \geq \sigma') \leq 2 \exp(-2\eta^2 n_{i,j} \sigma'^2), \tag{15}$$

where $\sigma' := \sigma/\eta$. Combining the results in inequalities (12) and (15) by letting σ' be $\frac{1}{\eta(n)} \sqrt{\frac{\alpha \ln T'}{n}}$ or $\frac{1}{\eta(n)} \sqrt{\frac{\alpha \ln n}{n}}$ in each term of (12), we further have

$$\begin{aligned}
P(\exists t \geq T', i, j, \mathcal{B}_{i,j}(t)) &\leq \sum_{i < j} \left[4 \sum_{n=0}^{T'} e^{-2\alpha \ln T'} + 2 \sum_{n=T'+1}^{\infty} e^{-2\alpha \ln n} \right] \\
&= \frac{K(K-1)}{2} \left[\sum_{n=1}^{T'} \frac{4}{T'^{2\alpha}} + \sum_{n=T'+1}^{\infty} \frac{2}{n^{2\alpha}} \right]. \tag{16}
\end{aligned}$$

This result align with that in (Zoghi et al. 2014). By treating n as a continuous variable, we can further bound it by

$$P(\exists t \geq T', i, j, \mathcal{B}_{i,j}(t)) \leq \frac{(4\alpha-1)K^2}{(2\alpha-1)T'^{2\alpha-1}}, \text{ with } T'^{2\alpha-1} > 0. \tag{17}$$

By setting $T' = C(\delta)$, inequality (4) holds, which completes the proof. \square

11.2 Calibration Threshold

Here we present the derivations of the ratio and the calibration threshold in equations (5) and (6).

Ratio of Confidence Intervals Considering $n_{i,j}^r(t) = 1$, at the t -th round, the uncertainty ratio of confidence bounds with and without a relative observation is

$$\frac{\hat{u}_{i,j} - \hat{l}_{i,j}}{\tilde{u}_{i,j} - \tilde{l}_{i,j}} = \frac{1}{\eta} \sqrt{\frac{\alpha \ln t}{n_{i,j}^d(t) + 1}} \cdot \sqrt{\frac{n_{i,j}^d(t)}{\alpha \ln t}} = \frac{1}{\eta} \sqrt{\frac{n_{i,j}^d(t)}{n_{i,j}^d(t) + 1}} = \sqrt{\frac{n_{i,j}^d(t)(n_{i,j}^d(t) + 1)}{(n_{i,j}^d(t) + w_{i,j}^r)^2}}. \tag{18}$$

This ratio is inversely proportional to $w_{i,j}^r$. For $w_{i,j}^r = 0$ and $w_{i,j}^r = 1$, we have

$$\begin{aligned} \sup \frac{\hat{u}_{i,j} - \hat{l}_{i,j}}{\tilde{u}_{i,j} - \tilde{l}_{i,j}} &= \sqrt{\frac{n_{i,j}^d(t) + 1}{n_{i,j}^d(t)}} = \sqrt{1 + \frac{1}{n_{i,j}^d(t)}}, \\ \inf \frac{\hat{u}_{i,j} - \hat{l}_{i,j}}{\tilde{u}_{i,j} - \tilde{l}_{i,j}} &= \sqrt{\frac{n_{i,j}^d(t)}{n_{i,j}^d(t) + 1}} = \sqrt{1 - \frac{1}{n_{i,j}^d(t) + 1}}, \end{aligned} \quad (19)$$

which indicates the interval in equation (5).

Calibration Threshold Given $n_{i,j}^d$ direct observations and $n_{i,j}^r$ related observations, we consider the case where a new related observations can be added. The ratio of interval with (denoted by $\hat{u}_{i,j}^1 - \hat{l}_{i,j}^1$ and η^1) and without (denoted by $\hat{u}_{i,j}^0 - \hat{l}_{i,j}^0$ and η^0) the added observation becomes:

$$\frac{\hat{u}_{i,j}^1 - \hat{l}_{i,j}^1}{\hat{u}_{i,j}^0 - \hat{l}_{i,j}^0} = \frac{\eta^0}{\eta^1} \sqrt{\frac{\alpha \ln t}{n_{i,j}(t) + 1}} \cdot \sqrt{\frac{n_{i,j}(t)}{\alpha \ln t}} = \frac{\eta^0}{\eta^1} \sqrt{\frac{n_{i,j}(t)}{n_{i,j}(t) + 1}} = \frac{\theta}{\theta + w_{i,j}^r} \sqrt{\frac{n_{i,j}(t) + 1}{n_{i,j}(t)}}, \quad (20)$$

where $\theta = \eta_0 n_{i,j}(t)$. To ensure a positive contribution, the ratio should less than 1, thus we have

$$\frac{\theta}{\theta + w_{i,j}^r} \sqrt{\frac{n_{i,j}(t) + 1}{n_{i,j}(t)}} \leq 1 \Rightarrow w_{i,j}^r \geq \theta \left(\sqrt{\frac{n_{i,j}(t) + 1}{n_{i,j}(t)}} - 1 \right) = \theta \left(\sqrt{1 + \frac{1}{n_{i,j}(t)}} - 1 \right), \quad (21)$$

which completes the derivation.

11.3 Sample Complexity: Proof of Theorem 3.2

Proof. For the case $i = j$, an arm cannot be played against itself with probability $1 - \delta$ when $t > C(\delta)$ according to Theorem 3.1. It is because when the first arm is selected as the first candidate in IPEA-RUCB, the second arm cannot be the same arm given the fact that $\hat{u}_{i,j} = 0.5 < p_{*,i} \leq \hat{u}_{*,i}$, $\forall t > C(\delta)$. This ensures that self-comparisons are avoided with high probability once the concentration condition holds. Consider the case where $i \neq j$. Let s be the last time a direct or related observation was added to the total observations of pair (a_i, a_j) , we have

$$\hat{u}_{i,j}(s) - \hat{l}_{i,j}(s) = \frac{2}{\eta} \sqrt{\frac{\alpha \ln s}{n_{i,j}}} \leq \sqrt{\frac{4\alpha \ln t}{\min_r w_{i,j}^{r,2} \cdot n_{i,j}}}. \quad (22)$$

The last inequality holds based on the fact that $w_{i,j}^r \in [0, 1]$ for all r , and

$$\eta = \frac{n_{i,j}^d + \sum_{k=1}^{n_{i,j}^r} w_{i,j}^k}{n_{i,j}} \geq \frac{\min_r w_{i,j}^r \cdot n_{i,j}^d + \sum_{k=1}^{n_{i,j}^r} \min_r w_{i,j}^r}{n_{i,j}} = \min_r w_{i,j}^r \frac{n_{i,j}^d + n_{i,j}^r}{n_{i,j}} = \min_r w_{i,j}^r.$$

Thus, suppose $n_{i,j} \geq D_{i,j}^w \ln t$ and $t > C(\delta)$ with $D_{i,j}^w$ defined in Theorem 3.2, we must have

$$\hat{u}_{i,j}(s) - \hat{l}_{i,j}(s) \leq \sqrt{\frac{4\alpha \ln t}{\min_r w_{i,j}^{r,2} \cdot n_{i,j}}} \leq \min\{\Delta_i^2, \Delta_j^2\}. \quad (23)$$

For a direct comparison of pair (a_i, a_j) , one of the following two scenarios must have happened:

Case 1 ($a_c = a_i$ and $a_d = a_j$) o include a_i in the candidate set \mathcal{C} , it must hold that $\hat{u}_{i,j}(s) \geq \frac{1}{2}$. Meanwhile, we have $\hat{l}_{i,j}(s) = 1 - \hat{u}_{j,i}(s) \leq 1 - p_{*,i}$. This follows from two conditions: i) $p_{*,i} \leq \hat{u}_{*,i}(t)$ when $t > C(\delta)$, and ii) if IPEA-RUCB chooses a_j as the most likely candidate to defeat a_i , we must have $\hat{u}_{*,i}(t) \leq \hat{u}_{j,i}(t)$. Combining these two inequalities yields:

$$\hat{u}_{i,j}(s) - \hat{l}_{i,j}(s) \geq \frac{1}{2} - (1 - p_{*,i}) = p_{*,i} - \frac{1}{2} = \Delta_i. \quad (24)$$

Case 2 ($a_c = a_j$ and $a_d = a_i$) By symmetry, swapping i and j in the above argument yields the corresponding result:

$$\hat{u}_{j,i}(s) - \hat{l}_{j,i}(s) \geq \frac{1}{2} - (1 - p_{*,j}) = \Delta_j. \quad (25)$$

These two scenarios yield $\hat{u}_{i,j} - \hat{l}_{i,j} \geq \max\{\Delta_i^2, \Delta_j^2\}$, which contradicts inequality (23). Therefore, with probability at least $1 - \delta$, it is not possible for $n_{i,j}$ to exceed both $C(\delta)$ and $D_{i,j}^w \ln t$. \square

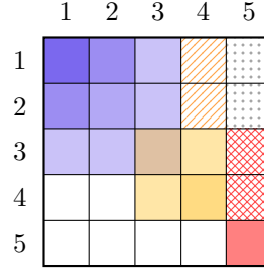


Figure 15: Illustration of soft clustering and regret decomposition. The color-filled regions represent intra-cluster groups: a_1, a_2, a_3, a_3, a_4 , and the singleton a_5 . The three line-patterned regions in the upper right correspond to inter-cluster comparisons with shared observations across related pairs.

11.4 Regret Analysis: Proof of Theorem 3.3

Proof. While the total sample complexity accounts for both direct and related observations, the cumulative regret is determined solely by direct observations. By definition, it is given by:

$$R(T) = \sum_{i,j \in \mathcal{A}, i < j} n_{i,j}^d(T) \cdot \frac{\Delta_i + \Delta_j}{2} \leq \sum_{i,j \in \mathcal{A}, i < j} n_{i,j}^d(T). \quad (26)$$

We decompose the cumulative regret $R(T)$ into multiple pair-level components, including inter-cluster pairs and intra-cluster comparisons among C possibly overlapped clusters. An illustrative example is provided in Figure 15 to facilitate understanding. For inter-cluster pairs, any two pairs belong to two distinct clusters share the same number of observations. For instance, the pairs (a_1, a_4) and (a_2, a_4) share the same observation count because a_1 and a_2 belong to the same cluster while a_4 belongs to a different one. This leads to the relation $n_{1,4} = n_{2,4}^d + n_{1,4}^d = n_{2,4}$. Consequently, inter-cluster regret can be reduced from a pairwise formulation to a cluster-level representation by avoiding repeated accounting of shared observations. Thus, for C clusters, the cluster-level component of the regret is effectively captured at the cluster level. For the remaining intra-cluster pairs, the regret is determined by the comparisons among the K_i arms within the i -th cluster.

Let $n(c_i, c_j)$ denote the total number of observations of all pairs spanning two clusters c_i and c_j . By performing this decomposition, the cumulative regret can be transformed as:

$$R(T) \leq \sum_{i,j \in \mathcal{A}, i < j} n_{i,j}^d(T) \leq \sum_{i,j \in \{1, \dots, C\}} n(c_i, c_j) + \sum_{c=1}^C \sum_{i,j \in c, i < j} n_{i,j}^d. \quad (27)$$

Note that the inequality sign reflects the potential overlap in the soft-clustering scenario.

We now study the regret bound for each component. For inter-cluster part, the cumulative regret is bounded as follows:

$$\sum_{i,j \in \{1, \dots, C\}, i < j} n(c_i, c_j) = \frac{C(C-1)}{2} \max_{i,j} D_{i,j}^w \ln t \Rightarrow \mathcal{O}\left(\frac{1}{\min_{i,j,r} w_{i,j}^r} C^2 \ln t\right). \quad (28)$$

For the remaining C intra-cluster components, if all regrets are counted, the cumulative regret can be bounded by $\sum_C \frac{K_i(K_i-1)}{2} \max_{i,j} D_{i,j}^w \ln t$. This bound follows from a microscopic view in which all arms are treated independently within their clusters. However, in IPEA-RUCB, candidates are selected not only based on intra-cluster winning times but also on global winning times. Therefore, for sub-optimal clusters that do not contain the winner a_* , the number of times that IPEA-RUCB selects pairs within the same cluster is bounded by a constant smaller than $C(\delta)$, as required to satisfy the concentration condition (Zoghi et al. 2014). As a result, the regret arising from intra-cluster comparisons is bounded by $\mathcal{O}\left(\frac{1}{\min_{i,j,r} w_{i,j}^r} \max_i K_i^2 \ln t\right)$. Combining both inter- and intra-cluster bounds yields the total cumulative regret bound as $\mathcal{O}\left(\frac{1}{\min_{i,j,r} w_{i,j}^r} \hat{K}^2 \ln t\right)$ where $\hat{K} = \max\{C, K_1, \dots, K_C\}$. \square

12 Broader impacts

Considering the broad development of personalization systems, IPE will play an important role in aligning system behavior with human preferences. With the foundational improvements proposed in our work, personalization systems can more efficiently capture and interpret user requirements, enabling better adaptation to individual needs. This capability is particularly critical in high-stakes applications such as healthcare and transportation, where humans are at the center of the system and alignment with their preferences can have lasting consequences.

At the same time, our work also raises potential negative impacts. The annotation of latent dependencies may introduce fairness and ethical concerns, particularly when such annotations reflect biased or offensive content. Care must be taken to ensure that the integration of contextual signals and richer forms of human feedback does not compromise equity or user trust.

13 Limitations

The proposed framework offers new insights into the design of DB algorithms, but several limitations remain that present opportunities for future work.

From a theoretical perspective, the current assumption of bidirectional dependency could be further relaxed to support more general dependency structures. Our analysis primarily focuses on deterministic strategies, and a more comprehensive theoretical investigation of stochastic strategies, such as IPEA-DTS, remains an open direction. Additionally, clearer principles for navigating the trade-off between efficiency and augmentation strength, either through refined regret analysis or conditions for uncertainty calibration, would provide stronger algorithmic guidance. For non-stationary preferences, an adaptive design to capture and respond to changes is also required (Yu et al. 2025; Yang, Lu, and Yu 2025).

From an algorithmic perspective, our prototype design could be enhanced in several ways, including the adoption of task-specific similarity metrics, more flexible in-context inference, and improved annotation strategies. In addition, given the potentially large space of dependencies, developing more efficient strategies and narrowing down the search space for acquiring them could substantially reduce computational costs (Wang and Li 2024). Moreover, the availability of benchmarks with richer forms of human feedback remains limited. Building such datasets would provide stronger validation for future research.

Lastly, our framework does not currently include explicit safeguards against annotation bias or misuse of feedback sources. This is particularly relevant when leveraging automated annotations from LLMs. Future work could explore the integration of robustness mechanisms to address these ethical and practical concerns in real-world deployment scenarios.

14 List of Notations

For convenience, we list the main notations used in this work in Table 4.

Table 4: Summary of the Main Mathematical Notation

| Symbol | Description |
|--|---|
| K | Total number of arms / candidates |
| C, c_i | Number of cluster with $C \leq K$, and the i -th cluster c_i |
| \mathcal{A} | Index set of arms from $\{1, \dots, K\}$ |
| a_* | Winner arm / best candidate |
| (a_i, a_j) | Pair of arm a_i and arm a_j , $i, j \in \mathcal{A}$ |
| $\mathbf{P} := [p_{i,j}]_{K \times K}$ | Preference matrix with winning probability of each pair $p_{i,j}$ |
| $\mathbf{B} := [b_{i,j}]_{K \times K}$ | Recorded winning matrix with $b_{i,j}$ the number of times a_i beats a_j |
| $\tilde{p}_{i,j}$ or $\hat{p}_{i,j}$ | Estimated mean of $p_{i,j}$, $\hat{p}_{i,j}$ includes augmented feedback |
| $\mathbf{U} := [\tilde{u}_{i,j} \text{ or } \hat{u}_{i,j}]_{K \times K}$ | Matrix of upper confidence bounds, \hat{u} denotes augmented bounds |
| $\mathbf{L} := [\tilde{l}_{i,j} \text{ or } \hat{l}_{i,j}]_{K \times K}$ | Matrix of lower confidence bounds, \hat{l} denotes augmented bounds |
| $x_i \in \mathcal{X}$ | Context vector x_i associated with a_i in the context space \mathcal{X} |
| $f(x_i, x_j)$ | Reward function of pair (a_i, a_j) associated with $x_i, x_j \in \mathcal{X}$ |
| θ | Unknown parameter in the reward function f |
| Δ_i | Difference from the best winning probability $p_{*,i} - \frac{1}{2}$ |
| t, T | Current iteration t and overall horizon of iterations T |
| $R(T) := \sum_{t=1}^T r_t$ | Cumulative regret over T rounds |
| α | Exploration coefficient |
| $n_{i,j}^d(t) := b_{i,j} + b_{j,i}$ | Number of direct observations of pair (a_i, a_j) up to time t |
| $n_{i,j}^r(t)$ | Number of related observations of pair (a_i, a_j) up to time t |
| $n_{i,j}(t)$ | Total count of observations (both direct and related) |
| $X_{i,j}^k$ | Random variable of the k -th related observation for pair (a_i, a_j) |
| $w_{i,j}^r$ | Dependency from the i -th related observation of pair (a_i, a_j) |
| η | Ratio $\eta = n_{i,j}^d + \sum_{i=1}^{n_{i,j}^r} w_{i,j}^k / n_{i,j}(t)$ |
| δ | Probability in concentration property |
| $C(\delta)$ | Upper bound of time for concentration $C(\delta) = \left(\frac{(4\alpha-1)K^2}{(2\alpha-1)\delta} \right)^{\frac{1}{2\alpha-1}}$ |
| $D_{i,j}^w$ | $D_{i,j}^w = 4\alpha \cdot (\min_r w_{i,j}^r)^2 \cdot \min\{\Delta_i^2, \Delta_j^2\})^{-1}$ |
| K_i | The i -th subset, $i \in \{1, \dots, C\}$ |
| \hat{K} | $\hat{K} = \max\{C, K_1, \dots, K_C\}$ |
| W | Dictionary of related observations |
| \mathcal{G} | Similarity graph from context |